HHS Public Access

Author manuscript

Biomaterials. Author manuscript; available in PMC 2017 March 01.

Published in final edited form as:

Biomaterials. 2016 March ; 83: 332–346. doi:10.1016/j.biomaterials.2016.01.020.

Evaluation of Cell-Laden Polyelectrolyte Hydrogels Incorporating Poly(L-Lysine) for Applications in Cartilage Tissue Engineering

Johnny Lam[1], **Elisa C. Clark**[1], **Eliza L.S. Fong**[1], **Esther J. Lee**[1], **Steven Lu**[1], **Yasuhiko Tabata**[2], and **Antonios G. Mikos**[1,*]

[1]Department of Bioengineering, Rice University, Houston, TX

[2]Department of Biomaterials, Institute of Frontier Medical Sciences, Kyoto University, Kyoto, Japan

Abstract

To address the lack of reliable long-term solutions for cartilage injuries, strategies in tissue engineering are beginning to leverage developmental processes to spur tissue regeneration. This study focuses on the use of poly(L-lysine) (PLL), previously shown to up-regulate mesenchymal condensation during developmental skeletogenesis *in vitro*, as an early chondrogenic stimulant of mesenchymal stem cells (MSCs). We characterized the effect of PLL incorporation on the swelling and degradation of oligo(poly(ethylene) glycol) fumarate) (OPF)-based hydrogels as functions of PLL molecular weight and dosage. Furthermore, we investigated the effect of PLL incorporation on the chondrogenic gene expression of hydrogel-encapsulated MSCs. The incorporation of PLL resulted in early enhancements of type II collagen and aggrecan gene expression and type II/type I collagen expression ratios when compared to blank controls. The presentation of PLL to MSCs encapsulated in OPF hydrogels also enhanced N-cadherin gene expression under certain culture conditions, suggesting that PLL may induce the expression of condensation markers in synthetic hydrogel systems. In summary, PLL can function as an inductive factor that primes the cellular microenvironment for early chondrogenic gene expression but may require additional biochemical factors for the generation of fully functional chondrocytes.

Keywords

hydrogel; poly(L-lysine); mesenchymal stem cells; condensation; chondrogenic differentiation; cartilage tissue engineering

[*]Corresponding Author: Antonios G. Mikos, Ph.D., Department of Bioengineering, Rice University, P.O. Box 1892, MS-142, Houston, TX 77251-1892, w: 713-348-5355, f: 713-348-4244, mikos@rice.edu.

1. Introduction

Articular cartilage is the specialized connective tissue that enables frictionless bone articulation within synovial joints in the body. Its elegantly organized extracellular matrix comprises specialized collagens and proteoglycans that together contribute to the favorable viscoelastic and swelling properties of the tissue. Unlike bone, articular cartilage is devoid of any vascularity, lymphatics, and nerves [1]. Due to this avascularity and the low mitotic activity of its resident chondrocytes, articular cartilage inherently exhibits a limited endogenous capacity for regeneration. In the absence of long-lasting clinical solutions, such cartilage-related injuries continue to impose a significant economic burden on society [2] and remain a leading cause of global disability [3, 4]. To address these shortcomings in the management of cartilage defects, current efforts are focused on the use of tissue engineering principles to develop better solutions.

By definition, hydrogels are three-dimensional (3D) polymer networks that consist of various hydrophilic components crosslinked to form water-insoluble matrices and have been investigated for applications in cartilage repair due to their highly favorable material properties [5]. These water-absorbent constructs can be fabricated from a wide variety of synthetic [6–9] or natural [10–16] materials for the encapsulation of mesenchymal stem cells (MSCs) and to provide *in vivo*-like conditions reminiscent of native articular cartilage microenvironments. While strategies aimed at maximizing their reparative capacity through the optimization of *in vitro* chondrogenic induction protocols have proven relatively successful [17–20], the ability to induce complete healing of damaged cartilage reliably [21] has not yet been achieved.

Recent strategies in cartilage tissue engineering are beginning to mimic specific stages in skeletogenesis with the goal of generating functional articular cartilage tissues [22–24]. Pre-cartilaginous condensation, a developmental process characterized by dense cellular aggregation and significantly increased cell-cell contacts, is believed to be critical in the governance of natural cartilage formation *in embryo* [25]. During condensation, the rapid onset of cell-cell interactions is largely mediated by a small number of key cell adhesion molecules, of which N-cadherin plays a special role [26–29]. Interestingly, previous research has demonstrated that the cationic polypeptide poly(L-Lysine) (PLL) possesses chondrostimulatory properties and can stimulate the chondrogenesis of mesenchymal micromass cells in developing chick limbs [30, 31]. Several mechanisms for the physiological effects of PLL on chondrogenic differentiation have been proposed, including alteration of glycosaminoglycan biosynthesis and distribution, crosslinking of proteoglycans and cells, changing of cell morphology, and interaction with other biochemical cues [27]. Despite these promising reports, the use of PLL to induce embryonic signaling processes during chondrogenesis in cartilage tissue engineering remains heavily unexplored, especially within the context of 3D culture systems.

In this study, we hypothesized that the physical incorporation of PLL within hydrogels can stimulate the chondrogenic gene expression of encapsulated MSCs. To test this hypothesis, we utilized oligo(poly(ethylene glycol) fumarate) (OPF), a PEG-based macromer that can be crosslinked to yield hydrolytically degradable hydrogels of highly tunable mechanical and

swelling properties [32, 33], as a synthetic platform to isolate the effects of PLL. Considering the cationic nature of PLL and the presence of negative charges from the OPF macromers comprising the hydrogel backbone, it is anticipated that both moieties will form strong electrostatic interactions, leading to the bulk retention of PLL. Further, it is expected that the incorporation of PLL will affect the swelling and degradation of these hydrogel constructs. In order to evaluate these hypotheses, a number of specific objectives were established as follows: (i) to determine the amount of PLL retained or released from OPF hydrogels when incorporated at various concentrations; (ii) to characterize the swelling and degradation of PLL-laden OPF hydrogels as functions of PLL molecular weight (MW) and PLL loading amount; (iii) to assess the effects of PLL incorporation on encapsulated MSC chondrogenic gene expression as functions of PLL MW and PLL dosage; and (iv) to evaluate potential additive or synergistic effects between PLL presentation and OPF MW on MSC chondrogenic gene expression and condensation.

2. Materials and Methods

2.1 Experimental Design

The specific objectives of this overall investigation were completed via a series of individual studies, which were designed as follows. In order to determine the amount of PLL retained or released from OPF hydrogels, two experiments were designed as outlined in Table 1. For a third experiment, fluorescein isothiocyanate (FITC) conjugated PLL (PLL-FITC, 50 kDa) was loaded into OPF hydrogels at increasing concentrations (500 ng/construct, 5 μg/construct, or 20 μg/construct) according to Table 2.

A full factorial study was designed to characterize the effects of PLL MW and PLL loading on the swelling and degradation of synthetic OPF hydrogels. Specifically, the factors of (A) PLL MW, (B) PLL loading per construct, and (C) OPF MW were investigated as outlined in Table 3 in order to identify main and combinatory effects on OPF swelling and degradation. The PLL MWs of 50 and 225 kDa were determined based on previously reported values used in the chondrogenic stimulation of chick limb mesenchymal cells in micromass culture *in vitro* [30]. The PLL loading concentrations were chosen to yield a sufficiently wide range in order to elucidate the effects of PLL on bulk hydrogel swelling, where the low concentration levels reflect those used for the chondrogenic stimulation of cells in monolayer [34].

The effects of PLL presentation on cells encapsulated in such composite hydrogels were also investigated. As shown in Table 4, the effects of PLL MW and PLL dosage on MSCs encapsulated in OPF hydrogel composites were first investigated using a factorial design, where the MW factor comprised two levels (50 or 225 kDa) and the dosage factor consisted of three levels (250 or 500 ng/construct). Cell-laden hydrogels without any PLL incorporation were used as negative controls. The PLL MW (225 kDa) and amount (500 ng/construct) yielding the highest chondrogenic gene expression in encapsulated MSCs were chosen in the follow-up experiment, which investigated any potential additive or synergistic effects of PLL presentation in combination with OPF MW on MSC chondrogenic gene expression as shown in Table 5. These OPF MWs were chosen based on a previous study from our laboratory, which demonstrated that an increase in swelling ratio (due to an

increase in nominal OPF MW from 10K to 35K) resulted in enhanced type II collagen gene expression [35].

2.2 OPF Synthesis and Characterization

OPF was synthesized using poly(ethylene glycol) (PEG) of nominal MWs of either 10,000 g/mol or 35,000 g/mol, according to previously described methods [32]. In brief, PEG was first dried via azeotropic distillation in toluene and dissolved in anhydrous dichloromethane. Triethylamine and fumaryl chloride were then added drop-wise to initiate the synthesis reaction, which was allowed to proceed for 2 days. The resultant product was purified by removing dichloromethane using rotoevaporation, separating salt precipitates with ethyl acetate, washing with ethyl ether, and subsequent drying. The synthesized polymers were characterized via gel permeation chromatography and sterilized prior to use by exposure to ethylene oxide gas for 12 h following established protocols [36].

2.3 Fabrication of PLL-laden Hydrogels

Acellular OPF hydrogels were fabricated following previously established procedures [37]. Briefly, a base formula of 100 mg OPF and 50 mg PEG diacrylate (PEG-DA, M_n 3,400 g/mol; Laysan, Arab, AL) dissolved in 410 μL of PBS was used to prepare the hydrogel precursor solution. For PLLladen hydrogels, PLL (Sigma Aldrich) of two different average MWs (either 50 kDa or 225 kDa) was dissolved in the polymer precursor solution at various concentrations prior to crosslinking in order to achieve the desired incorporation amounts per construct (250 or 500 ng/construct). For the OPF-Post samples of the PLL retention study, a PLL solution was used to rehydrate crosslinked hydrogels that were dried immediately following the removal of sol fraction in PBS for 2 h in order to achieve the desired loading concentration. The two different average MWs of PLL were chosen in accordance to previous studies demonstrating the effect of PLL size on cartilage nodule formation in micromass cultures of chick mesenchyme limb bud cells, where larger PLL size generally increased tissue formation [30]. These concentrations were chosen to reflect similar PLL concentrations that have been previously used for the chondrogenic stimulation of mesenchymal derived cells in monolayer [30, 34]. Equal parts (46.8 μL) of the thermal radical initiators, 0.3 M of ammonium persulfate (APS, Sigma Aldrich) and 0.3 M of *N,N,N',N'* – tetramethylethylenediamine (TEMED, Sigma Aldrich) were then added to the precursor solution to initiate the crosslinking reaction. After gentle mixing, the precursor solution was quickly injected into cylindrical Teflon molds (3 mm diameter and 1 mm thickness) and allowed to crosslink for 8 min at 37°C. The resultant hydrogels were transferred to PBS (pH 7.4), incubated at room temperature or 37°C for 28 days, and collected at various time points over 28 days for characterization.

2.4 Swelling and Degradation of OPF-PLL Hydrogels

Fabricated hydrogels for the swelling and degradation study (n=4) were placed in 2 mL of PBS (pH 7.4) in a 24 well plate and incubated at 37°C and under agitation (shaker table at 90–100 RPM) for 28 days. At days 1, 7, 14, and 28, the swelling ratio and mass loss of the hydrogels were determined using the following equations: swelling ratio = $(W_s - W_d)/W_d$ and % mass loss = $(W_i - W_d)/W_i \times 100$ (%), where W_i, W_s, and W_d represent the weight of

dried hydrogel immediately following fabrication before swelling, the weight of wet hydrogel after swelling at each time point, and the weight of dried hydrogel after swelling at each time point, respectively.

2.5 Measurement of PLL Retention in OPF-PLL Hydrogels

Briefly, blank OPF hydrogels, OPF hydrogels with PLL loaded prior to hydrogel crosslinking (OPF-Pre), and OPF hydrogels with PLL loaded after hydrogel fabrication (OPF-Post) were incubated after the removal of sol fraction in either phosphate buffered saline (PBS, pH 7.4) or a KCl/NaOH basic buffer (pH 13) for 24 h at 37°C. At 2 h and 24 h, the supernatant is collected from each sample (n=3) and subjected to biochemical analysis. In order to characterize PLL retention within OPF hydrogels over longer periods of time *in vitro*, blank OPF and OPF-Pre samples were incubated in PBS over 28 days at 37°C. At 2 h, 24 h, 7 days, 14 days, and 21 days, samples (n=3) were switched to basic buffer and incubated for 24 h before collection, where the resultant supernatant was then analyzed for PLL.

The amount of PLL retained was biochemically analyzed using the *ortho*-pthalaldehyde (OPA) assay according to previously established procedures [38, 39]. The OPA working reagent was freshly prepared at each time point following a base formula by mixing 1 mL of OPA (Sigma Aldrich) dissolved in ethanol (40 mg/mL), 25 mL borate buffer (0.4 M borate, pH 9.5), 12.5 mL 20 w/w% sodium dodecyl sulfate (Sigma Aldrich) in deionized water, 0.1 mL 2-mercaptoethanol, and enough water to fill up to 50 mL in a beaker. The supernatants were combined with the OPA working reagent within individual wells of an opaque 96-well plate at a 1:1 reagent-to-analyte solution ratio and incubated at room temperature for 5 min. The fluorescence was measured using a plate reader (FL x800 Fluorescence Microplate Reader; BioTek Instruments, Winooski, VT) with excitation and emission wavelengths of 360 nm and 455 nm, respectively. PLL of the same MW was used to generate a standard curve.

PLL-FITC laden constructs (n=3) were incubated in PBS over 28 days at room temperature. The supernatant was collected at .08 (2 h), 1, 4, 7, 11, 14, 18, 21, 25, and 28 days and analyzed using a spectrofluorometric plate reader with respective excitation and emission wavelengths of 485 nm and 528 nm to determine the release of PLL.

2.6 Gelatin Microparticle Fabrication

Gelatin microparticles (GMPs) were fabricated using acidic gelatin with an isoelectric point of 5.0 (Nitta Gelatin Inc., Osaka, Japan) according to previously established protocols [40]. Briefly, a 10% w/v aqueous solution of gelatin was first prepared by dissolving 5 g of gelatin in 45 mL of distilled, deionized water (ddH_2O) at 60°C, added dropwise to 250 mL of olive oil (Sigma Aldrich) containing 0.5 wt.% Span 80 under mixing at 500 RPM, and chilled in an ice/water bath for 30 min with continued mixing. 100 mL of chilled acetone was then added to the emulsion, which was allowed to stir for an additional 30 min. After this step, the formed GMPs were collected by filtration and washed with acetone. The collected GMPs were crosslinked in an aqueous solution containing 10 mM glutaraldehyde for 20 h at 15°C, where glycine was added to a concentration of 25 mM afterward in order to

quench any unreacted glutaraldehyde. Following crosslinking, the GMPs were vacuum-filtered, washed with ddH_2O, and freeze-dried overnight. Dried GMPs of 50–100 μm in diameter were selected by sieving and sterilized via exposure to ethylene oxide gas for 12 h before use. Prior to encapsulation into hydrogels, sterilized GMPs were first swollen with PBS (55 μL of PBS per 11 mg of dried GMPs) to achieve swelling according to previously established methods [40]. It was previously shown that GMPs encapsulated within OPF hydrogel composites improved chondrocyte proliferation [41] and enabled cell aggregation when compared to blank hydrogel controls, indicating improved cell-material interactions [36]. As such, GMPs were incorporated into hydrogels in order to provide moieties for cell-material interactions and to facilitate hydrogel degradation [42, 43].

2.7 Rabbit Marrow-derived MSC Isolation and Culture

All of the experimental protocols including the use of cells for this study were reviewed and approved by the Rice University Institutional Animal Care and Use Committee, and conducted in accordance with the National Institutes of Health animal care and use guidelines. Rabbit marrow-derived MSCs were harvested from the tibiae of six skeletally mature 6-month-old male New Zealand White rabbits following previously described protocols [19]. The bone marrow was plated for the isolation of adherent cells and cultured in general medium (GM) containing low glucose Dulbecco's modified Eagle's medium (LG-DMEM), 10% v/v fetal bovine serum (FBS), and 1% v/v penicillin/streptomycin/fungizone (PSF) for 2 weeks. Non-adherent cells were removed during routine media changes. The rabbit marrow-derived MSCs were then pooled together (from six total rabbits) to minimize interanimal variation and then cryopreserved until use as previously described [19, 42, 43]. For MSC expansion and hydrogel encapsulation in studies involving cell-laden constructs, cryopreserved cells were thawed at 37 °C and cultured at a density of 3,500 cells per cm^2 in T-225 tissue culture flasks in GM up to passage three, at which point a cell suspension is prepared for hydrogel encapsulation.

2.8 Fabrication of Cell-laden Hydrogel Composites

The procedures for the fabrication of acellular OPF hydrogels were generally followed for the fabrication of cell-laden hydrogel composites with a few exceptions. Specifically, 100 mg OPF and 50 mg PEG-DA were both dissolved in 300 μL of PBS and combined with 110 μL of swollen GMPs to generate the polymer precursor solution. Equal parts of thermal radical initiator solutions APS and TEMED were then added as previously described. After mixing of the precursor solution to initiate the crosslinking reaction for 2–3 min, a cell suspension (6.7 million cells in 168 μL of PBS) of MSCs is then added in order to obtain a final concentration of 10 million cells per mL and gently mixed. The solution was then quickly injected into cylindrical Teflon molds (6.0 mm diameter and 1.0 mm thickness) and incubated at 37°C for 8 min to complete crosslinking.

After fabrication, cell-laden hydrogel constructs were transferred to individual wells of a 24-well plate and cultured in 2 mL of serum-free chondrogenic medium (CM) containing LG-DMEM, ITS+ Premix (6.25 μg/mL insulin, 6.25 μg/mL transferrin, 6.25 μg/mL selenious acid, 5.35 μg/mL linoleic acid, and 1.25 μg/mL bovine serum albumin) (Corning, Corning NY), 50 mg/L ascorbic acid, 10^{-7} M dexamethasone, and 1% v/v PSF for up to 28 days. No

chondrogenic growth factors were included in the medium in order to isolate the effects of PLL alone on chondrogenic gene expression. For the experiment described, the CM was supplemented with β-glycerophosphate (β-GP) in order in investigate the chondrogenic as well as mineralization potential of encapsulated MSCs. The medium was changed every 3 days. At each prescribed time point (0, 7, 14, or 28 days), samples were retrieved from tissue culture and collected for biochemical assays (n=4) and quantitative real-time polymerase chase reaction (n=4).

2.9 Real-Time Reverse Transcriptase Polymerase Chain Reaction (RT-PCR)

Cell-laden hydrogel composites were processed for RT-PCR in order to quantify the expression of selected genes as indicators of chondrogenic differentiation. Total RNA from collected samples were isolated at various time points using the RNeasy Mini Kit (Qiagen, Valencia, CA) following established protocols [19]. The isolated RNA from samples were reverse-transcribed into cDNA using SuperScript III transcriptase (Invitrogen) and Oligo dT primers (Promega), and the final cDNA transcripts were used for RT-PCR (7300 Real-Time PCR System, Applied Biosystems, Foster City, CA) to evaluate the gene expression for type II collagen (Col II), type I collagen (Col I), aggrecan (Agg), versican (VSN), sex-determining region Y-box 9 (Sox9), N-cadherin (CDH2), type X collagen (Col X), and glyceraldehyde-3-phosphate dehydrogenase (GAPDH). The gene expression data were analyzed using the $2^{-\Delta\Delta Ct}$ method as described [44, 45]. All gene expression data were normalized to that of the housing keeping gene, GAPDH, and are expressed as the fold ratio as compared to the baseline expression of the control group at day 0. For the experiments described in this study, the control group comprised the cell-laden 10K OPF samples without any PLL incorporation, which were analyzed immediately following cell encapsulation. The primer sequences used are listed in Table 6.

2.10 Biochemical Assays

At each time point, cell-laden hydrogel samples were collected and frozen in −20°C until use for biochemical analysis. Samples were thawed, homogenized via needle and syringe, and digested in 500 μL of proteinase K solution (1 mg/mL proteinase K, 0.01 mg/mL pepstatin A and 0.185 mg/mL iodoacetamide dissolved in 50 mM tris(hydroxymethyl aminomethane)/1 mM ethylenediaminetetraacetic acid buffer, pH 7.6 adjusted by HCl) at 56°C for ~16 h. After the digestion of samples, specimens were then subjected to three freeze-thaw cycles followed by probe sonication.

DNA content, which was used as an indicator of construct cellularity, was quantified using the Quant-iT PicoGreen dsDNA Assay Kit (Molecular Probes, Eugene, OR) following the manufacturer's instructions. Cell lysates were combined with assay buffer and the PicoGreen dye solution within wells of an opaque 96-well assay plate and allowed to incubate for 10 min at room temperature. The fluorescence was quantified using excitation and emission wavelengths of 485 nm and 528 nm (FL x800 Fluorescence Microplate Reader; BioTek Instruments, Winooski, VT), respectively. Lambda DNA provided by the manufacturer was used to generate a standard curve.

Glycosaminoglycan (GAG) content, which was used to indicate extracellular matrix deposition and synthetic activity, was measured using the dimethylmethylene blue (DMMB) colorimetric assay as previously described [46]. Cell lysates were combined with DMMB color reagent within wells of a clear 96-well assay plate and quantified for absorbance at 520 nm (PowerWave x340 Microplate Reader; BioTek Instruments). GAG concentrations were determined relative to a chondroitin sulfate standard curve. To determine the synthetic activity of cells within the hydrogel constructs, the resulting total GAG amounts from each sample were normalized to the total DNA amount from that sample.

Hydroxyproline (HYP) content, which was used to indicate total collagen amount and synthetic activity, was determined using a colorimetric assay following previously established protocols [19]. Cell lysates were combined with an equal volume of 4 N NaOH and hydrolyzed via autoclave for 15 min at 121°C (~50 min processing time). The resultant solutions were neutralized with HCl and acetic acid to pH 6.5–7.0 and divided into duplicate reactions. Chloramine-T, followed by *p*-dimethylaminobenzaldehyde solutions, was subsequently added and the absorbance at 570 nm was measured with a plate reader. The HYP concentrations were measured relative a standard curve generated using *trans*-4-hydroxy-L-proline. To determine the collagen synthetic activity of cells within the hydrogel constructs, the resulting total HYP amounts from each sample were divided by the total DNA amount from that sample. Due to the presence of GMPs in cell-laden hydrogels, which comprise denatured collagen, HYP/DNA values for each group were also normalized to day 0 HYP/DNA values for that same group in order to evaluate changes in collagen synthetic activity.

The calcium content was measured to assess the propensity of stimulated MSCs to undergo hypertrophic endochondral ossification. Acetic acid was added to cell lysates to achieve a final acidic concentration of 0.5 M for all samples, which were then allowed to incubate at room temperature overnight. This releases calcium from the homogenized cell-laden hydrogel composites. The calcium content was then quantified using a colorimetric assay. In brief, treated samples were combined with calcium arsenazo III reagent (Sekisui Diagnostics, Lexington, MA) and the absorbance was measured at 650 nm using a plate reader. The calcium concentrations were determined relative to a calcium chloride standard curve. Calcium concentrations were then normalized to the day 0 values within each group in order to characterize mineralization capacity over time.

2.11 Histology

Cell-laden OPF hydrogel composites were fixed for histology in 10% neutral buffered formalin (Fisher Scientific, Pittsburg, PA), soaked in a solution of phosphate-buffered saline with 15% sucrose to prevent rapid water crystal formation, and then embedded overnight in HistoPrep freezing medium (Fisher Scientific). After freezing, blocks were sectioned into 10–15 μm thick slices using a cryostat (Leica CM 1850 UW; Leica Biosystems Nussloch GmbH, Germany) and mounted onto glass slides. Sections were stained using Alcian Blue and Fast Green in order to visualize the extracellular matrix deposition and cell distribution, respectively. Bright-field images were obtained using a light microscope equipped with a

digital camera attachment for image capture (Axio Imager.Z2 with AxioCam MRc5; Carl Zeiss MicroImaging GmbH, Germany).

2.12 Statistical Analysis

All results are presented as means ± standard deviations. Statistical analysis of all data was performed using the SAS JMP Pro 11 software package. For the PLL release data, the swelling and degradation data, and the biochemical assay data, one-way ANOVA and Tukey's HSD multiple comparison tests were performed to determine significant differences between groups. The RT-PCR data were analyzed using the Kruskal-Wallis test following by the Mann-Whitney U test to determine significant differences between groups [48, 49]. A confidence interval of 95% was utilized and differences were considered significant when $p<0.05$.

3. Results

3.1 Retention and Release of PLL from PLL-laden OPF Hydrogels

We hypothesized that cationic PLL would undergo strong ionic interactions with the electronegative carboxyl moieties on the OPF backbone when incorporated into OPF hydrogels. However, the addition of PLL during the hydrogel crosslinking process could also potentially result in addition reactions between the pendant amines on PLL and the unsaturated carbon-carbon double bonds on the fumarate blocks of OPF. To determine the mechanism of the interactions between PLL and OPF, the first retention experiment compared blank OPF hydrogels (OPF) to OPF hydrogels with PLL loaded during crosslinking (OPF-Pre) and to OPF hydrogels with PLL loaded after crosslinking (OPF-Post), where the OPF-Post hydrogels were generated by swelling dried hydrogels in a PLL-containing solution. In analyzing the supernatant from each group in PBS (pH 7.4) after 24 h using the detection of primary amines as an indirect measure of PLL, we found that PLL was detected only in the OPF-Post group (Figure 1a). Notably, when the supernatants were analyzed from parallel experimental groups incubated in basic buffer (pH 13) after 24 h, PLL was detected for both OPF-Pre and OPF-Post groups. Additionally, significantly more PLL was detected in the supernatant of the OPF-Pre group in basic conditions when compared to the OPF-Pre supernatants at neutral pH (Figure 1b).

Next, to evaluate the retention of PLL within OPF hydrogels over longer durations, OPF and OPF-Pre hydrogels were incubated at neutral pH in PBS over 21 days. Comparing the sol fractions after 2 h, higher levels of primary amines were detected in the OPF control group, likely due to the presence of amine groups from the thermal radical initiators (APS and TEMED) used for chemical crosslinking (Figure 1c). Subsequently, at 7, 14, and 21 days, no PLL was detected in the supernatant of the OPF-Pre group. Following the collection of the supernatant at each time point, hydrogel samples were transferred to basic buffer and incubated for an additional 24 h in order to release any retained PLL into the supernatant. Higher levels of primary amines were detected in the supernatant of the OPF-Pre group as compared to the OPF group at days 1, 7, and 21, suggesting that PLL was indeed retained within the hydrogels and subsequently released in basic conditions (Figure 1d).

The release of PLL from PLL-laden hydrogels as influenced by the initial PLL loading concentration was further characterized using FITC conjugated PLL (PLL-FITC). The cumulative release profiles of PLL-FITC from OPF-500ng, OPF-5μg, and OPF-20μg hydrogels are shown in Figures 2a and 2b. Each PLL-laden group exhibited an initial burst release at 2 h ranging from 1% to 7% of the initial loading amount, where higher amounts of PLL-FITC loaded initially resulted in a greater burst release. Following the burst release, the amount of PLL-FITC released from all PLL-laden groups stabilized by day 28 to approximately 14% of the initial loading amount for the 10K hydrogels and up to 25% for the 35K hydrogels. Specifically, the amount of PLL-FITC released translates into an 84.1%, 86.0%, and 83.9% retention of the loaded PLL-FITC for OPF-500ng, OPF-5μg, and OPF-20μg 10K hydrogels, respectively. 75.0%, 81.8%, and 76.5% of the loaded PLL-FITC was retained for OPF-500ng, OPF-5μg, and OPF-20μg 35K hydrogels, respectively. To visualize the incorporation of PLL-FITC within the hydrogels, hydrogel samples were collected at 7 and 28 days and imaged using fluorescence microscopy. Higher fluorescent intensities were observed for groups incorporating higher amounts of PLL-FITC (Figure2c and 2d). Decreased fluorescence from the incorporated PLL-FITC at later time points were likely a result of the degradation of the FITC signal. Indeed, the PLL-FITC stock used to generate the standard curve for the analysis of released PLL exhibited decreased fluorescent signals over time at ambient temperature.

3.2 Characterization of the Swelling Behavior and Degradation of OPF Hydrogels Incorporating PLL of Varying Size and Loading Amount

Given that the PLL was largely retained within OPF hydrogels over the timeframe evaluated, the influence of PLL on the swelling behavior and degradation of OPF hydrogels was also investigated using the formulations outlined in Table 3. The mean equilibrium swelling ratios, as affected by PLL MW, PLL incorporation, and PLL dosage, were first compared between 10K OPF hydrogels (Figure 3a). At day 1, both formulations incorporating high MW PLL, 10K225Hi and 10K225Lo, and the formulation containing a high amount of low MW PLL, 10K50Hi, exhibited greater swelling ratios when compared to the control group. At day 7, 10K225Lo hydrogels had higher swelling ratios when compared to 10K225Hi hydrogels and blank 10K controls. By day 28, however, the blank 10K control hydrogels and 10K50Lo hydrogels maintained the highest equilibrium swelling ratios, where the former was greater than the 10K50Hi formulations and the latter was greater when compared to both the 10K50Hi and 10K225Lo formulations.

A comparison of the equilibrium swelling ratios between 35K OPF hydrogels (Figure 3b) revealed similar differences between groups as those observed for their 10K counterparts. Specifically, 35K225Hi, 35K225Lo, and 35K50Hi hydrogels initially exhibited greater equilibrium swelling ratios when compared to 35K control hydrogels at day 1; both 35K225 formulations also maintained higher swelling ratios when compared to 35K50Lo hydrogels at this time point. Unlike their 10K hydrogel counterparts, 35K225Hi, 35K225Lo, and 35K50Lo had lower swelling ratios when compared to 35K50Hi and blank 35K control hydrogels as early as day 7. At day 14, 35K225Hi hydrogels retained the lowest swelling ratios when compared to 35K50Hi, 35K225Lo, and blank 35K hydrogels. By day 28, blank 35K hydrogels retained the highest equilibrium swelling ratios when compared to all PLL-

laden formulations with the exception of 35K225Lo hydrogels, which swelled more than those from 35K225Hi and 35K50Lo formulations.

Differences in mass loss manifested between 10K formulations only at the early time points of days 1 and 7 (Figure 3c). At day 1, 10K50Lo hydrogels maintained the lowest initial mass loss when compared to all other groups except for 10K225Lo hydrogels. At day 7, both 10K50Lo and 10K225Hi hydrogels had the least mass loss when compared to all other groups. The only differences in mass loss observed between 35K hydrogel formulations occurred at day 7, where 35K225Hi and blank 35K control hydrogels had more mass loss than 35K50Hi hydrogels (Figure 3d). The mean swelling ratio and mass loss data, as well as a formal main effects analysis of the data, are presented in Reference [47].

3.3 Effects of PLL Loading, PLL MW, and PLL Dosage on the Chondrogenic Gene Expression of Encapsulated MSCs

MSCs were encapsulated in OPF hydrogels using the formulations outlined in Table 4, where hydrogels without any PLL incorporated served as the negative control. These cell-laden hydrogels from the first cell study were cultured in defined chondrogenic media supplemented with β-GP in order to investigate their chondrogenic as well as mineralization potential. First, assessment of cell viability at 24 h and 7 days following hydrogel encapsulation indicated that cells remained viable and that the incorporation of PLL did not negatively affect cell viability [47]. We have also previously shown that MSCs encapsulated in OPF hydrogel composites remained viable over 28 days of culture *in vitro* [42].

The influence of PLL MW and dosage on the chondrogenic gene expression of encapsulated MSCs was then evaluated at an early (day 7) and late (day 28) time point. With the exception of the type II/type I collagen fold ratio, the effects of PLL on chondrogenic gene expression were largely observed at day 7. Specifically, the incorporation of 225 kDa PLL resulted in increased type II collagen gene expression at both loading dosages when compared to the control (Figure 4a). This effect was not observed for 50 kDa PLL. Interestingly, the incorporation of 50 kDa PLL at 250 ng per construct led to a decrease in type II collagen expression at day 7 when compared to the control group. By day 28, all groups exhibited similar type II collagen expression levels, which were expected from MSCs encapsulated in synthetic hydrogel systems. In considering the fold ratio of type II to type I collagen, only 225 kDa PLL incorporated at 500 ng per construct elicited increases in the fold expression ratio, which was reflective of decreases in type I collagen expression, that was sustained over 28 days when compared to all other groups (Figure 4b). Notably, 50 kDa PLL at both loading concentrations (250 and 500 ng per construct) resulted in initial decreases in type II/type I collagen fold ratio at day 7 when compared to the control. This is likely the result of both decreased type II collagen expression and increased type I collagen expression. By day 28, however, type II/type I collagen fold ratios were similar for all groups with the exception of the group incorporating 225 kDa PLL at 500 ng per construct.

In addition to size dependent effects of PLL on the type II collagen gene expression and type II/type I collagen fold ratio, dosage dependent effects were observed particularly in formulations containing PLL of higher MW (225 kDa). Specifically, the incorporation of PLL at 500 ng per construct resulted in the highest aggrecan expression as compared to the

250 ng per construct and the control groups (Figure 4c). Lastly, the mineralization of these cell-laden hydrogels as influenced by the incorporation of PLL was also investigated. The amounts of calcium were normalized to day 0 values within each group in order to reflect the mineralization capacity of hydrogels from each of the formulations tested, and hence, do not necessarily depict total calcium amounts. The incorporation of PLL, regardless of size or loading amount, inhibited increases in mineralization over time (Figure 4d). Indeed, only hydrogels from the control group showed increased normalized calcium when compared to all other PLL-laden hydrogels at both days 7 and 28.

3.4 Effects of PLL Presentation in Combination With OPF MW on the Chondrogenic Gene Expression and Condensation Signaling of Encapsulated MSCs

From the study above, we determined that the incorporation of 225 kDa PLL within cell-laden OPF hydrogels at a loading concentration of 500 ng per construct produced the greatest effect on chondrogenic gene expression without enhancing mineralizing potential. Based on our previous observation that hydrogels fabricated from OPF of higher MW can enhance the chondrogenic gene expression of encapsulated cells [35], we sought to evaluate the effect of PLL incorporation (using the optimized parameters above) in combination with varying OPF MW (10 or 35K) on the cellularity, synthetic activity, and chondrogenic gene expression of encapsulated MSCs (Table 5). These hydrogels were cultured in serum-free and defined chondrogenic medium without β-GP nor external growth factors over 28 days in vitro in order to isolate the effects of PLL presentation on MSC chondrogenic gene expression in synthetic hydrogels.

As shown in Figure 5a, using DNA content as an indicator of cellularity, a decrease in DNA content after day 0 was initially observed for all groups, which is typically expected from the encapsulation of cells in synthetic hydrogel systems [42, 43]. DNA levels were then stabilized within each group for most formulations following day 7 with the exception of 35K PLL-laden hydrogels, which experienced a slight increase in cellularity following day 14. By day 28, 10K PLL-laden hydrogels maintained the lowest DNA content when compared to all other groups.

In evaluating GAG synthetic activity, we found that the incorporation of PLL led to increased GAG deposition in cell-laden 10K OPF but not 35K OPF hydrogel composites at day 14. Indeed, 10K OPF hydrogels loaded with PLL were the only experimental group that displayed increases in GAG synthetic activity from encapsulation until day 14, after which their normalized GAG values decreased (Figure 5b). For the analysis of the collagen synthetic activity, HYP/DNA values were normalized to the day 0 values within each group in order to elucidate increases in collagen synthetic activity over time as well as factor out the collagen content associated with the encapsulated GMPs. Similarly for collagen synthetic activity, differences between groups were again only observed at day 14, where both the 10K and 35K OPF groups containing PLL displayed increased collagen deposition when compared to their respective non-PLL loaded counterparts (Figure 5c). Furthermore, PLL-laden hydrogels fabricated with 10K OPF macromers exhibited enhanced activity when compared to those fabricated with 35K OPF macromers. Such an effect was not observed between the two non-PLL containing groups. Histological sections for GAG and collagen

showed slight increases in staining for the 10K or both the 10K and 35K PLL-laden groups, respectively (Figure 6).

In addition to the biochemical analyses, the type II collagen and aggrecan gene expression, and the type II/type I collagen expression ratio were evaluated as indicators of chondrogenic differentiation. Within defined culture conditions, changes in OPF MW (as opposed to PLL loading) appeared to dominate trends in type II collagen gene expression. PLL-laden 35K OPF hydrogels displayed enhanced type II collagen expression when compared to their corresponding 10K OPF counterparts at both early and late time points (Figure 7a). Some transient changes in type II collagen expression were observed at day 14 as a result of both increasing OPF MW and PLL incorporation. For aggrecan, while the inclusion of PLL into 10K OPF hydrogels enhanced expression levels at day 7, this was not observed for the 35K hydrogels (Figure 7b). Notably, aggrecan expression levels were similarly increased for both 35K OPF groups when compared to the 10K OPF controls. Similar to the trends observed for type II collagen, the aggrecan gene expression fluctuated after day 7 with the 10K OPF control group expressing the highest levels of aggrecan at day 14. By day 28, all groups exhibited comparable aggrecan gene expression, highlighting an early effect of PLL on chondrogenic gene expression. Lastly, the type II/type I collagen fold ratio was also evaluated as an indicator of hyaline-like or fibrocartilage-like differentiation. While there appeared to be no additive or synergistic effects between the factors of PLL incorporation or OPF MW on MSC chondrogenic gene expression within culture conditions free of external stimuli including growth factors and β-GP, the inclusion of PLL stimulated increases in type II/type I fold ratios at day 7 for 35K OPF hydrogels and at day 28 for 10K OPF hydrogels (Figure 7c).

In addition to the standard chondrogenic markers described above, we also analyzed the gene expression levels of Sox9, VSN, type X collagen, and CDH2. Although there were no differences in gene expression levels observed between groups for both Sox9 and VSN at early or late time points, the addition of PLL into OPF hydrogels appeared to affect some changes at day 14 (Figures 8a and 8b). Interestingly, the inclusion of PLL within 10K OPF hydrogels actually resulted in a decrease in both Sox9 and VSN gene expression at intermediate times. However, differences in Sox9 and VSN expression were no longer present by day 28. For type X collagen gene expression, the expression levels for all groups were generally below the detection threshold from day 7 forward. To evaluate any possible effects of PLL on the condensation signaling of encapsulated MSCs, CDH2 gene expression was also assessed. Similar to type II collagen expression, changes in CDH2 expression were primarily influenced by the factor of OPF MW. MSCs encapsulated in 35K OPF hydrogel composites without PLL displayed lower CDH2 expression after day 7 when compared to both 10K OPF formulations (Figure 8c). While initially lower when compared to the 10K OPF groups at day 7, the CDH2 expression levels of PLL-laden 35K OPF hydrogels increased over time and exhibited similar values by day 28. Importantly, the incorporation of PLL effected an increase in CDH2, and hence N-cadherin, expression, which was observed between the 35K OPF groups at day 28 (Figure 8c).

4. Discussion

To address the limited regenerative potential of current cartilage engineering strategies, it is theorized that the induction of developmental processes can instruct host or transplanted cells to adopt native morphogenetic programs for robust tissue regeneration [50, 51]. During condensation, increased cell-cell interactions mediated by cell-cell adhesion molecules (such as N-cadherin) [52, 53] permit the exchange of chondrogenic signals between cells [27, 54–56]. Indeed, it has been previously shown that the functionalization of hydrogels with N-cadherin mimetic peptides was sufficient to stimulate the chondrogenic differentiation of encapsulated MSCs [57]. In a different approach, early studies have demonstrated that the treatment of chick mesenchymal micromasses with soluble PLL elicited a size- and dose-dependent response on cartilage nodule formation [30] and have shown that PLL promotes chondrogenesis via the upregulation of functional N-cadherin expression [31]. Whether PLL can exert chondro-stimulatory effects in a three-dimensional context, however, still remains to be investigated. By successfully leveraging these properties of PLL, especially given its ubiquity in biomedical technologies, one can potentially provide a clinically relevant way of implementing an effective developmental approach for cartilage tissue regeneration.

In the present study, we hypothesized that the incorporation of PLL polypeptides into synthetic OPF hydrogel systems, in addition to influencing hydrogel swelling and degradation properties, will stimulate the chondrogenic gene expression of encapsulated MSCs. We found that PLL remained largely retained within OPF hydrogels when incorporated during hydrogel fabrication despite differences in the initial loading concentration. The retention of PLL is likely due to the formation of a tight interpenetrating network held together via electrostatic interactions between the cationic polypeptide and electronegative groups with partial negative charges (i.e. carbonyl groups) on the OPF polymer backbone. Incorporation and retention of cationic PLL within hydrogels also resulted in ionization of the resultant constructs, which affected their swelling behavior and degradation. Characterization of hydrogel swelling at early time points generally showed that PLL-laden constructs initially exhibited greater swelling ratios when compared to blank controls. Typically, swelling of a neutral biopolymer hydrogel network is largely governed by the thermodynamic compatibility of the solute (i.e. the polymer chains) with the aqueous solvent and the rubber elasticity of the polymer chains as described by the Flory-Rehner theory [58]. When the polymer chains are ionized, however, the presence of polymer-polymer charge interactions can also significantly influence hydrogel swelling behavior, where like charges support swelling while opposite charges hinder swelling [59–61]. The incorporation of cationic PLL polypeptides into OPF hydrogels introduced a surplus of positively charged moieties that led to an initial repulsion of similarly charged polymer chains in the interpenetrating network. Over time, hydrolytic degradation of the OPF polymer chains yielded negatively charged moieties in the form of carboxylic acids and oligomerized fumaric acids [32, 62] that possess an electrostatic affinity for cationic groups. Subsequent affinity between the interpenetrating PLL and OPF chains opposes hydrogel swelling, which was observed at later time points in the swelling study where PLL-laden groups generally swelled less in comparison to controls.

Regarding hydrogel degradation, it was anticipated that the electrostatic interactions between the sol fraction and incorporated PLL would lead to a reduction in initial mass loss. While the differentiating trends in mass loss amongst the varying hydrogel formulations were generally minor, blank OPF hydrogels of both 10K and 35K OPF MW both did display greater mass loss than some PLL-laden groups at early time points up until day 7. Such changes in hydrogel swelling behavior and degradation suggest that PLL can be leveraged for the generation of hydrogel constructs with desirable dynamic swelling properties for cartilage engineering applications.

We also evaluated the chondrogenic gene expression of encapsulated MSCs as effected by PLL size and loading dosage. From our results, we showed that PLL primarily stimulated the expression of chondrogenic gene markers at early time points, where dose-dependent effects were mainly discerned for aggrecan expression and size-dependent effects were mainly detected for type II collagen expression. The induction of hyaline-like MSC chondrogenic gene expression profiles as a result of PLL presentation was most evident in the type II/type I collagen expression ratio. The PLL225–500 group induced the highest chondrogenic type II/type I collagen gene expression ratios of MSCs encapsulated within OPF hydrogels when compared to all other groups. As this was due in large part to a decrease in type I collagen gene expression for the PLL225–500 group, these results suggest that PLL may inhibit chondrogenic dedifferentiation of MSCs in such hydrogel systems. Previously, it was only shown that PLL promoted increases in chondrogenic gene expression of MSCs in monolayer [34]. Here, we show that PLL can also induce the chondrogenic gene expression of MSCs encapsulated within hydrogels. However, the chondrogenic differentiation of MSCs *in vitro* typically does not arrest at the chondrocyte stage and often leads to hypertrophy followed by subsequent formation of calcified tissues that are detrimental to the function of articular cartilage [63]. Interestingly, all PLL-laden groups exhibited decreased calcium accumulation over time when compared to the negative control. This could possibly be attributed to the cationic forces of the incorporated PLL inhibiting the nucleation of positively charged calcium within these cell-laden constructs via electrostatic repulsion.

To further investigate the chondro-stimulatory properties of PLL within the context of a well-established hydrogel system, we hypothesized (in our second cell encapsulation study) that the effects of PLL would work synergistically with increases in OPF MW toward enhancing the chondrogenic synthetic activity and gene expression of encapsulated MSCs. However, we did not observe any combinatory effects of PLL and OPF MW on chondrogenic gene expression under the conditions investigated. For the biochemical characterization, overall construct cellularity decreased after encapsulation and stabilized for the duration of culture as expected [19, 36, 42, 43]. PLL incorporation significantly heightened both the GAG and collagen synthetic activity, especially at intermediate time points. However, the buildup of detectable extracellular matrix diminished following day 14, likely as a result of overall construct degradation. Although the exact mechanism of PLL's stimulatory effects on chondrogenesis still remains to be determined, it was established that PLL promoted the pericellular retention of proteoglycans as well as other anionic extracellular matrix components, allowing for cumulative extracellular matrix assembly and

subsequent cartilage nodule formation [64]. Given that a synthetic hydrogel system was employed for our studies to isolate the effects of PLL, we did not expect to observe significant extracellular matrix deposition over time since other more potent growth factors were not incorporated. This outcome was indicated in the histology, which also suggests PLL's early effects on chondrogenic gene expression. While not investigated here, data from the present study would be enhanced with additional analyses characterizing the production of extracellular matrix components specific to articular cartilage, such as type II collagen.

In elucidating the effect of OPF MW and PLL incorporation on chondrogenic gene expression, we found that increases OPF MW generally enhanced gene expression, which corroborates previous results from our laboratory [35]. While both PLL-laden and PLL-free 35K OPF composites also exhibited heightened aggrecan expression when compared to 10K OPF controls early on, we found that the incorporation of PLL to 10K OPF hydrogels also enhanced their early aggrecan expression. Further analysis of the type II/type I collagen expression ratio confirmed that incorporation of PLL into OPF hydrogel composites indeed enhanced the hyaline-like chondrogenic gene expression of encapsulated MSCs. Although no direct assessments were made in the present study, comparison of the gene expression data from the two cell encapsulation experiments suggests that β-GP played a role in facilitating the stimulatory effects of PLL on chondrogenic gene expression. Since β-GP is known to stimulate the osteogenic differentiation of MSCs via increasing alkaline phosphatase activity and altering local phosphate ion concentrations [65, 66], there may exist some interplay between β-GP and PLL that influences both bone and cartilage development, since both processes are preceded by condensation *in embryo* [25]. This particular phenomenon, although not researched in the current study, warrants further investigation.

As a proteoglycan that shares common features with aggrecan, versican is thought to play a prevalent role in the regulation of extracellular matrix assembly during pre-cartilaginous condensation [67, 68]. Additionally, sox9 is understood to be essential for cartilage formation [69] and is often considered an early chondrogenic marker. Cells encapsulated within these hydrogels did not undergo hypertrophy as indicated by the inability to detect (below detection threshold) any type X collagen gene expression. Furthermore, the absence of any discernable trends in versican and sox9 gene expression as a result of PLL incorporation highly suggests that PLL may have likely stimulated chondrogenesis via an indirect mechanism through N-cadherin. Notably, we detected an increase in N-cadherin expression for 35K OPF hydrogel composites at day 28 as a result of PLL incorporation when compared to the PLL-free 35K control, which corroborates previously reported data; Woodward and Tuan found that PLL stimulates the chondrogenic differentiation of mesenchymal micromass cultures by upregulating functional N-cadherin expression, both of which are essential for promoting pre-cartilaginous condensation [31]. However, differences in temporal N-cadherin expression patterns when compared to 2D cultures indicate that the incorporation parameters of PLL in 3D hydrogels, such as size and dosage, may require further optimization in order to accurately recapitulate proper conditions for condensation. While PLL does not exist naturally *in vivo* [27], its ability to interact with cells intracellularly as well as though their extracellular matrix [31] suggest the existence of

biological counterparts to PLL. PLL has indeed been thought to mimic the chondrogenesis-promoting actions of procollagen and fibronectin, both of which contain cationic regions similar to PLL [27, 64, 70–72]. Whether or not PLL adopts similar mechanisms in promoting chondrogenic differentiation in 3D hydrogel systems requires further study. Additionally, the chondrostimulatory effects of PLL should also be confirmed *in vivo* using an orthotopic animal model in future investigations. Interestingly, decreasing OPF MW also appeared to increase N-cadherin expression in MSCs encapsulated in OPF hydrogel systems. This phenomenon could be attributed to increases in hydrogel osmotic pressure due to decreases in MW between crosslinked chains as described by the Flory-Rehner theory [5, 58, 73–75], which would likely simulate the physical cues present as a result of dense cell-cell interactions during pre-cartilaginous condensation [76, 77].

5. Conclusion

In summary, we developed a 3D hydrogel platform incorporating PLL as an inductive factor for stimulating the chondrogenesis of encapsulated MSCs. Upon loading into synthetic hydrogels, PLL remains largely retained where it is capable of exerting size- and dose-dependent changes on the swelling behavior and degradation of the resultant composite constructs. We demonstrate that the incorporation of PLL into synthetic OPF hydrogels dynamically influences their swelling behavior, which may be leveraged for the development of constructs with desirable dynamic swelling properties for cartilage tissue engineering applications. Within these hydrogel composites, PLL also stimulated early gene expression of MSCs, in which higher MW and loading amounts resulted in greater chondrogenic gene expression. Additionally, the incorporation of PLL also promoted an increase in N-cadherin expression under certain conditions. Together, our results demonstrate that PLL can function as an inductive factor that primes the cellular microenvironment for early chondrogenic gene expression but may require additional stimulatory factors for the generation of fully functional chondrocytes. By leveraging these chondro-stimulatory properties of PLL, notably given its ubiquity in biomedical technologies, we provide herein a clinically relevant and developmental-inspired strategy for cartilage tissue regeneration.

Acknowledgments

This study was supported by the National Institutes of Health (R01 AR048756 and R01 AR068073).

References

1. Sophia Fox AJ, Bedi A, Rodeo SA. The basic science of articular cartilage: structure, composition, and function. Sports health. 2009; 1:461–468. [PubMed: 23015907]
2. Behery O, Siston RA, Harris JD, Flanigan DC. Treatment of cartilage defects of the knee: expanding on the existing algorithm. Clinical journal of sport medicine : official journal of the Canadian Academy of Sport Medicine. 2014; 24:21–30. [PubMed: 24157464]
3. Cross M, Smith E, Hoy D, Carmona L, Wolfe F, Vos T, et al. The global burden of rheumatoid arthritis: estimates from the global burden of disease 2010 study. Annals of the rheumatic diseases. 2014; 73:1316–1322. [PubMed: 24550173]

4. Cross M, Smith E, Hoy D, Nolte S, Ackerman I, Fransen M, et al. The global burden of hip and knee osteoarthritis: estimates from the global burden of disease 2010 study. Annals of the rheumatic diseases. 2014; 73:1323–1330. [PubMed: 24553908]
5. Slaughter BV, Khurshid SS, Fisher OZ, Khademhosseini A, Peppas NA. Hydrogels in Regenerative Medicine. Adv Mater. 2009; 21:3307–3329. [PubMed: 20882499]
6. Bryant SJ, Anseth KS. Hydrogel properties influence ECM production by chondrocytes photoencapsulated in poly(ethylene glycol) hydrogels. Journal of biomedical materials research. 2002; 59:63–72. [PubMed: 11745538]
7. Bryant SJ, Arthur JA, Anseth KS. Incorporation of tissue-specific molecules alters chondrocyte metabolism and gene expression in photocrosslinked hydrogels. Acta biomaterialia. 2005; 1:243–252. [PubMed: 16701801]
8. Bryant SJ, Davis-Arehart KA, Luo N, Shoemaker RK, Arthur JA, Anseth KS. Synthesis and characterization of photopolymerized multifunctional hydrogels: Water-soluble poly(vinyl alcohol) and chondroitin sulfate macromers for chondrocyte encapsulation. Macromolecules. 2004; 37:6726–6733.
9. Lee CT, Kung PH, Lee YD. Preparation of poly(vinyl alcohol)-chondroitin sulfate hydrogel as matrices in tissue engineering. Carbohyd Polym. 2005; 61:348–354.
10. Chen X, Zhang F, He X, Xu Y, Yang Z, Chen L, et al. Chondrogenic differentiation of umbilical cord-derived mesenchymal stem cells in type I collagen-hydrogel for cartilage engineering. Injury. 2013; 44:540–549. [PubMed: 23337703]
11. Choi B, Kim S, Lin B, Wu BM, Lee M. Cartilaginous extracellular matrix-modified chitosan hydrogels for cartilage tissue engineering. ACS applied materials & interfaces. 2014; 6:20110–20121. [PubMed: 25361212]
12. Eyrich D, Brandl F, Appel B, Wiese H, Maier G, Wenzel M, et al. Long-term stable fibrin gels for cartilage engineering. Biomaterials. 2007; 28:55–65. [PubMed: 16962167]
13. Kim IL, Mauck RL, Burdick JA. Hydrogel design for cartilage tissue engineering: a case study with hyaluronic acid. Biomaterials. 2011; 32:8771–8782. [PubMed: 21903262]
14. Mierisch CM, Cohen SB, Jordan LC, Robertson PG, Balian G, Diduch DR. Transforming growth factor-beta in calcium alginate beads for the treatment of articular cartilage defects in the rabbit. Arthroscopy : the journal of arthroscopic & related surgery : official publication of the Arthroscopy Association of North America and the International Arthroscopy Association. 2002; 18:892–900.
15. Toh WS, Lim TC, Kurisawa M, Spector M. Modulation of mesenchymal stem cell chondrogenesis in a tunable hyaluronic acid hydrogel microenvironment. Biomaterials. 2012; 33:3835–3845. [PubMed: 22369963]
16. Wakitani S, Goto T, Young RG, Mansour JM, Goldberg VM, Caplan AI. Repair of large full-thickness articular cartilage defects with allograft articular chondrocytes embedded in a collagen gel. Tissue engineering. 1998; 4:429–444. [PubMed: 9916174]
17. Fisher MB, Henning EA, Soegaard NB, Dodge GR, Steinberg DR, Mauck RL. Maximizing cartilage formation and integration via a trajectory-based tissue engineering approach. Biomaterials. 2014; 35:2140–2148. [PubMed: 24314553]
18. Lam J, Lu S, Lee EJ, Trachtenberg JE, Meretoja VV, Dahlin RL, et al. Osteochondral defect repair using bilayered hydrogels encapsulating both chondrogenically and osteogenically predifferentiated mesenchymal stem cells in a rabbit model. Osteoarthritis and cartilage / OARS, Osteoarthritis Research Society. 2014; 22:1291–1300.
19. Lam J, Lu S, Meretoja VV, Tabata Y, Mikos AG, Kasper FK. Generation of osteochondral tissue constructs with chondrogenically and osteogenically predifferentiated mesenchymal stem cells encapsulated in bilayered hydrogels. Acta biomaterialia. 2014; 10:1112–1123. [PubMed: 24300948]
20. Mauck RL, Yuan X, Tuan RS. Chondrogenic differentiation and functional maturation of bovine mesenchymal stem cells in long-term agarose culture. Osteoarthritis and cartilage / OARS, Osteoarthritis Research Society. 2006; 14:179–189.

21. Anderson JA, Little D, Toth AP, Moorman CT 3rd, Tucker BS, Ciccotti MG, et al. Stem cell therapies for knee cartilage repair: the current status of preclinical and clinical studies. The American journal of sports medicine. 2014; 42:2253–2261. [PubMed: 24220016]
22. Bhumiratana S, Eton RE, Oungoulian SR, Wan LQ, Ateshian GA, Vunjak-Novakovic G. Large, stratified, and mechanically functional human cartilage grown in vitro by mesenchymal condensation. Proc Natl Acad Sci U S A. 2014; 111:6940–6945. [PubMed: 24778247]
23. Ghone NV, Grayson WL. Recapitulation of mesenchymal condensation enhances in vitro chondrogenesis of human mesenchymal stem cells. Journal of cellular physiology. 2012; 227:3701–3708. [PubMed: 22378248]
24. Wu L, Bluguermann C, Kyupelyan L, Latour B, Gonzalez S, Shah S, et al. Human developmental chondrogenesis as a basis for engineering chondrocytes from pluripotent stem cells. Stem cell reports. 2013; 1:575–589. [PubMed: 24371811]
25. Hall BK, Miyake T. All for one and one for all: condensations and the initiation of skeletal development. BioEssays : news and reviews in molecular, cellular and developmental biology. 2000; 22:138–147.
26. Ahrens PB, Solursh M, Reiter RS. Stage-related capacity for limb chondrogenesis in cell culture. Developmental biology. 1977; 60:69–82. [PubMed: 198274]
27. DeLise AM, Fischer L, Tuan RS. Cellular interactions and signaling in cartilage development. Osteoarthritis and cartilage / OARS, Osteoarthritis Research Society. 2000; 8:309–334.
28. Oberlender SA, Tuan RS. Spatiotemporal profile of N-cadherin expression in the developing limb mesenchyme. Cell adhesion and communication. 1994; 2:521–537. [PubMed: 7743138]
29. Tavella S, Raffo P, Tacchetti C, Cancedda R, Castagnola P. N-CAM and N-cadherin expression during in vitro chondrogenesis. Experimental cell research. 1994; 215:354–362. [PubMed: 7982473]
30. San Antonio JD, Tuan RS. Chondrogenesis of limb bud mesenchyme in vitro: stimulation by cations. Developmental biology. 1986; 115:313–324. [PubMed: 2423399]
31. Woodward WA, Tuan RS. N-Cadherin expression and signaling in limb mesenchymal chondrogenesis: stimulation by poly-L-lysine. Developmental genetics. 1999; 24:178–187. [PubMed: 10079520]
32. Kinard LA, Kasper FK, Mikos AG. Synthesis of oligo(poly(ethylene glycol) fumarate). Nature protocols. 2012; 7:1219–1227. [PubMed: 22653160]
33. Lam J, Kim K, Lu S, Tabata Y, Scott DW, Mikos AG, et al. A factorial analysis of the combined effects of hydrogel fabrication parameters on the in vitro swelling and degradation of oligo(poly(ethylene glycol) fumarate) hydrogels. Journal of biomedical materials research Part A. 2014; 102:3477–3487. [PubMed: 24243766]
34. Lu H, Guo L, Kawazoe N, Tateishi T, Chen G. Effects of poly(L-lysine), poly(acrylic acid) and poly(ethylene glycol) on the adhesion, proliferation and chondrogenic differentiation of human mesenchymal stem cells. Journal of biomaterials science Polymer edition. 2009; 20:577–589. [PubMed: 19323877]
35. Park H, Guo X, Temenoff JS, Tabata Y, Caplan AI, Kasper FK, et al. Effect of swelling ratio of injectable hydrogel composites on chondrogenic differentiation of encapsulated rabbit marrow mesenchymal stem cells in vitro. Biomacromolecules. 2009; 10:541–546. [PubMed: 19173557]
36. Park H, Temenoff JS, Tabata Y, Caplan AI, Mikos AG. Injectable biodegradable hydrogel composites for rabbit marrow mesenchymal stem cell and growth factor delivery for cartilage tissue engineering. Biomaterials. 2007; 28:3217–3227. [PubMed: 17445882]
37. Kim K, Lam J, Lu S, Spicer PP, Lueckgen A, Tabata Y, et al. Osteochondral tissue regeneration using a bilayered composite hydrogel with modulating dual growth factor release kinetics in a rabbit model. Journal of controlled release : official journal of the Controlled Release Society. 2013; 168:166–178. [PubMed: 23541928]
38. Grotzky A, Manaka Y, Fornera S, Willeke M, Walde P. Quantification of alpha-polylysine: a comparison of four UV/Vis spectrophotometric methods. Anal Methods-Uk. 2010; 2:1448–1455.
39. Harris JD, Taylor GA, Blake TK, Sands DC. A Fluorometric Assay for Determining Variation of Lysine in Wheat Gliadin Proteins. Euphytica. 1994; 76:97–100.

40. Holland TA, Tabata Y, Mikos AG. In vitro release of transforming growth factor-beta 1 from gelatin microparticles encapsulated in biodegradable, injectable oligo(poly(ethylene glycol) fumarate) hydrogels. Journal of controlled release : official journal of the Controlled Release Society. 2003; 91:299–313. [PubMed: 12932709]
41. Park H, Temenoff JS, Holland TA, Tabata Y, Mikos AG. Delivery of TGF-beta1 and chondrocytes via injectable, biodegradable hydrogels for cartilage tissue engineering applications. Biomaterials. 2005; 26:7095–7103. [PubMed: 16023196]
42. Guo X, Liao J, Park H, Saraf A, Raphael RM, Tabata Y, et al. Effects of TGF-beta 3 and preculture period of osteogenic cells on the chondrogenic differentiation of rabbit marrow mesenchymal stem cells encapsulated in a bilayered hydrogel composite. Acta biomaterialia. 2010; 6:2920–2931. [PubMed: 20197126]
43. Guo X, Park H, Liu GP, Liu W, Cao YL, Tabata Y, et al. In vitro generation of an osteochondral construct using injectable hydrogel composites encapsulating rabbit marrow mesenchymal stem cells. Biomaterials. 2009; 30:2741–2752. [PubMed: 19232711]
44. Livak KJ, Schmittgen TD. Analysis of relative gene expression data using real-time quantitative PCR and the 2(−Delta Delta C(T)) Method. Methods. 2001; 25:402–408. [PubMed: 11846609]
45. Schmittgen TD, Livak KJ. Analyzing real-time PCR data by the comparative C(T) method. Nature protocols. 2008; 3:1101–1108. [PubMed: 18546601]
46. Farndale RW, Buttle DJ, Barrett AJ. Improved quantitation and discrimination of sulphated glycosaminoglycans by use of dimethylmethylene blue. Biochimica et biophysica acta. 1986; 883:173–177. [PubMed: 3091074]
47. Lam J, Clark EC, Fong ELS, Lee EJ, Lu S, Tabata Y, et al. Data to support the evaluation of cell-laden polyelectrolyte hydrogels incorporating poly(L-lysine) for applications in cartilage tissue engineering. Data-in-Brief. 2015 Submitted.
48. Dahlin RL, Ni M, Meretoja VV, Kasper FK, Mikos AG. TGF-beta3-induced chondrogenesis in co-cultures of chondrocytes and mesenchymal stem cells on biodegradable scaffolds. Biomaterials. 2014; 35:123–132. [PubMed: 24125773]
49. Meretoja VV, Dahlin RL, Kasper FK, Mikos AG. Enhanced chondrogenesis in co-cultures with articular chondrocytes and mesenchymal stem cells. Biomaterials. 2012; 33:6362–6369. [PubMed: 22695067]
50. Occhetta P, Centola M, Tonnarelli B, Redaelli A, Martin I, Rasponi M. High-Throughput Microfluidic Platform for 3D Cultures of Mesenchymal Stem Cells, Towards Engineering Developmental Processes. Scientific reports. 2015; 5:10288. [PubMed: 25983217]
51. Scotti C, Piccinini E, Takizawa H, Todorov A, Bourgine P, Papadimitropoulos A, et al. Engineering of a functional bone organ through endochondral ossification. Proc Natl Acad Sci U S A. 2013; 110:3997–4002. [PubMed: 23401508]
52. DeLise AM, Tuan RS. Alterations in the spatiotemporal expression pattern and function of Ncadherin inhibit cellular condensation and chondrogenesis of limb mesenchymal cells in vitro. Journal of cellular biochemistry. 2002; 87:342–359. [PubMed: 12397616]
53. Delise AM, Tuan RS. Analysis of N-cadherin function in limb mesenchymal chondrogenesis in vitro. Developmental dynamics : an official publication of the American Association of Anatomists. 2002; 225:195–204. [PubMed: 12242719]
54. Coelho CN, Kosher RA. A gradient of gap junctional communication along the anterior-posterior axis of the developing chick limb bud. Developmental biology. 1991; 148:529–535. [PubMed: 1743400]
55. Coelho CN, Kosher RA. Gap junctional communication during limb cartilage differentiation. Developmental biology. 1991; 144:47–53. [PubMed: 1995401]
56. Zimmermann B. Assembly and disassembly of gap junctions during mesenchymal cell condensation and early chondrogenesis in limb buds of mouse embryos. Journal of anatomy. 1984; 138(Pt 2):351–363. [PubMed: 6715255]
57. Bian LM, Guvendiren M, Mauck RL, Burdick JA. Hydrogels that mimic developmentally relevant matrix and N-cadherin interactions enhance MSC chondrogenesis. P Natl Acad Sci USA. 2013; 110:10117–10122.

58. Peppas NA, Huang Y, Torres-Lugo M, Ward JH, Zhang J. Physicochemical foundations and structural design of hydrogels in medicine and biology. Annual review of biomedical engineering. 2000; 2:9–29.
59. Ostroha J, Pong M, Lowman A, Dan N. Controlling the collapse/swelling transition in charged hydrogels. Biomaterials. 2004; 25:4345–4353. [PubMed: 15046925]
60. Podual K, Doyle FJ, Peppas NA. Preparation and dynamic response of cationic copolymer hydrogels containing glucose oxidase. Polymer. 2000; 41:3975–3983.
61. Wiese KG, Heinemann DE, Ostermeier D, Peters JH. Biomaterial properties and biocompatibility in cell culture of a novel self-inflating hydrogel tissue expander. Journal of biomedical materials research. 2001; 54:179–188. [PubMed: 11093177]
62. Timmer MD, Shin H, Horch RA, Ambrose CG, Mikos AG. In vitro cytotoxicity of injectable and biodegradable poly(propylene fumarate)-based networks: unreacted macromers, cross-linked networks, and degradation products. Biomacromolecules. 2003; 4:1026–1033. [PubMed: 12857088]
63. Dickhut A, Pelttari K, Janicki P, Wagner W, Eckstein V, Egermann M, et al. Calcification or dedifferentiation: requirement to lock mesenchymal stem cells in a desired differentiation stage. Journal of cellular physiology. 2009; 219:219–226. [PubMed: 19107842]
64. San Antonio JD, Jacenko O, Yagami M, Tuan RS. Polyionic regulation of cartilage development: promotion of chondrogenesis in vitro by polylysine is associated with altered glycosaminoglycan biosynthesis and distribution. Developmental biology. 1992; 152:323–335. [PubMed: 1644223]
65. Boskey AL, Guidon P, Doty SB, Stiner D, Leboy P, Binderman I. The mechanism of beta-glycerophosphate action in mineralizing chick limb-bud mesenchymal cell cultures. J Bone Miner Res. 1996; 11:1694–1702. [PubMed: 8915777]
66. Martin I, Padera RF, Vunjak-Novakovic G, Freed LE. In vitro differentiation of chick embryo bone marrow stromal cells into cartilaginous and bone-like tissues. J Orthopaed Res. 1998; 16:181–189.
67. Kamiya N, Watanabe H, Habuchi H, Takagi H, Shinomura T, Shimizu K, et al. Versican/PG-M regulates chondrogenesis as an extracellular matrix molecule crucial for mesenchymal condensation. Journal of Biological Chemistry. 2006; 281:2390–2400. [PubMed: 16257955]
68. Varghese S, Hwang NS, Canver AC, Theprungsirikul P, Lin DW, Elisseeff J. Chondroitin sulfate based niches for chondrogenic differentiation of mesenchymal stem cells. Matrix biology : journal of the International Society for Matrix Biology. 2008; 27:12–21. [PubMed: 17689060]
69. Bi WM, Deng JM, Zhang ZP, Behringer RR, de Crombrugghe B. Sox9 is required for cartilage formation. Nat Genet. 1999; 22:85–89. [PubMed: 10319868]
70. Frenz DA, Jaikaria NS, Newman SA. The mechanism of precartilage mesenchymal condensation: a major role for interaction of the cell surface with the amino-terminal heparin-binding domain of fibronectin. Developmental biology. 1989; 136:97–103. [PubMed: 2806726]
71. Obrink B. The influence of glycosaminoglycans on the formation of fibers from monomeric tropocollagen in vitro. European journal of biochemistry / FEBS. 1973; 34:129–137. [PubMed: 4267112]
72. Obrink B, Laurent TC, Carlsson B. The binding of chondroitin sulphate to collagen. FEBS letters. 1975; 56:166–169. [PubMed: 1157930]
73. Flory PJ, Rehner J. Statistical mechanics of cross-linked polymer networks II Swelling. J Chem Phys. 1943; 11:521–526.
74. Flory PJ, Rehner J. Statistical mechanics of cross-linked polymer networks I Rubberlike elasticity. J Chem Phys. 1943; 11:512–520.
75. Hooper HH, Baker JP, Blanch HW, Prausnitz JM. Swelling Equilibria for Positively Ionized Polyacrylamide Hydrogels. Macromolecules. 1990; 23:1096–1094.
76. Cao B, Li Z, Peng R, Ding J. Effects of cell-cell contact and oxygen tension on chondrogenic differentiation of stem cells. Biomaterials. 2015; 64:21–32. [PubMed: 26113183]
77. Cao LP, Cao B, Lu CJ, Wang GW, Yu L, Ding JD. An injectable hydrogel formed by in situ crosslinking of glycol chitosan and multi-benzaldehyde functionalized PEG analogues for cartilage tissue engineering. J Mater Chem B. 2015; 3:1268–1280.

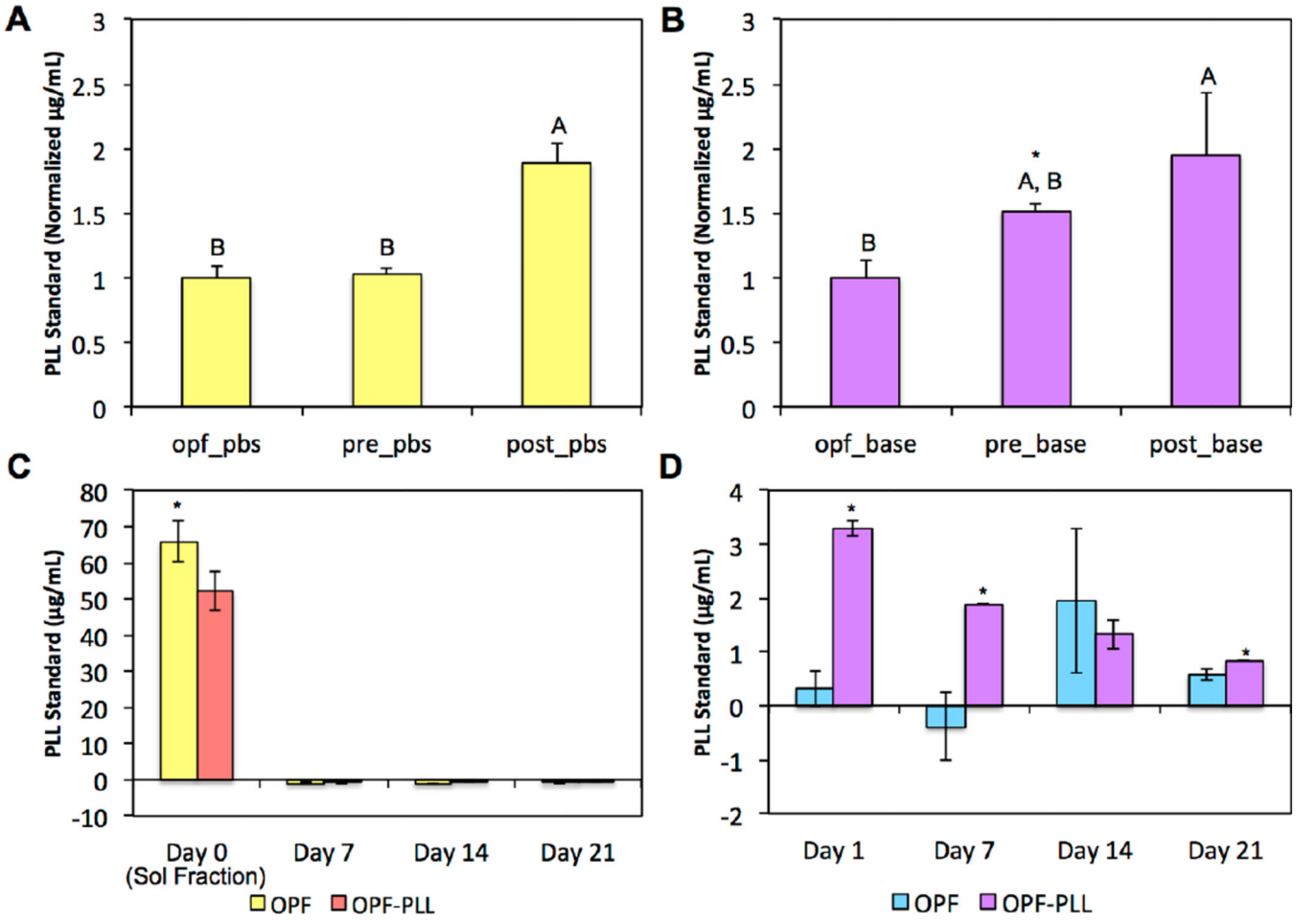

Figure 1.

An indirect measure of PLL retention through the detection of released PLL is shown in (A) PBS (pH 7.4) or in (B) basic buffer (pH 13) after 24 h between OPF controls, OPF hydrogels loaded with PLL during fabrication (pre), and OPF hydrogels loaded with PLL after fabrication (post). Within each incubation condition, groups not connected by the same letters are significantly different ($p < 0.05$). Within each group, * indicates a difference between incubation conditions. Released PLL is shown in (C) PBS and in (D) basic buffer over 21 days between OPF-PLL and blank controls. At each time point for (C) and (D), the * indicates a significant difference between groups ($p<0.05$). Error bars represent the standard deviation (n=3).

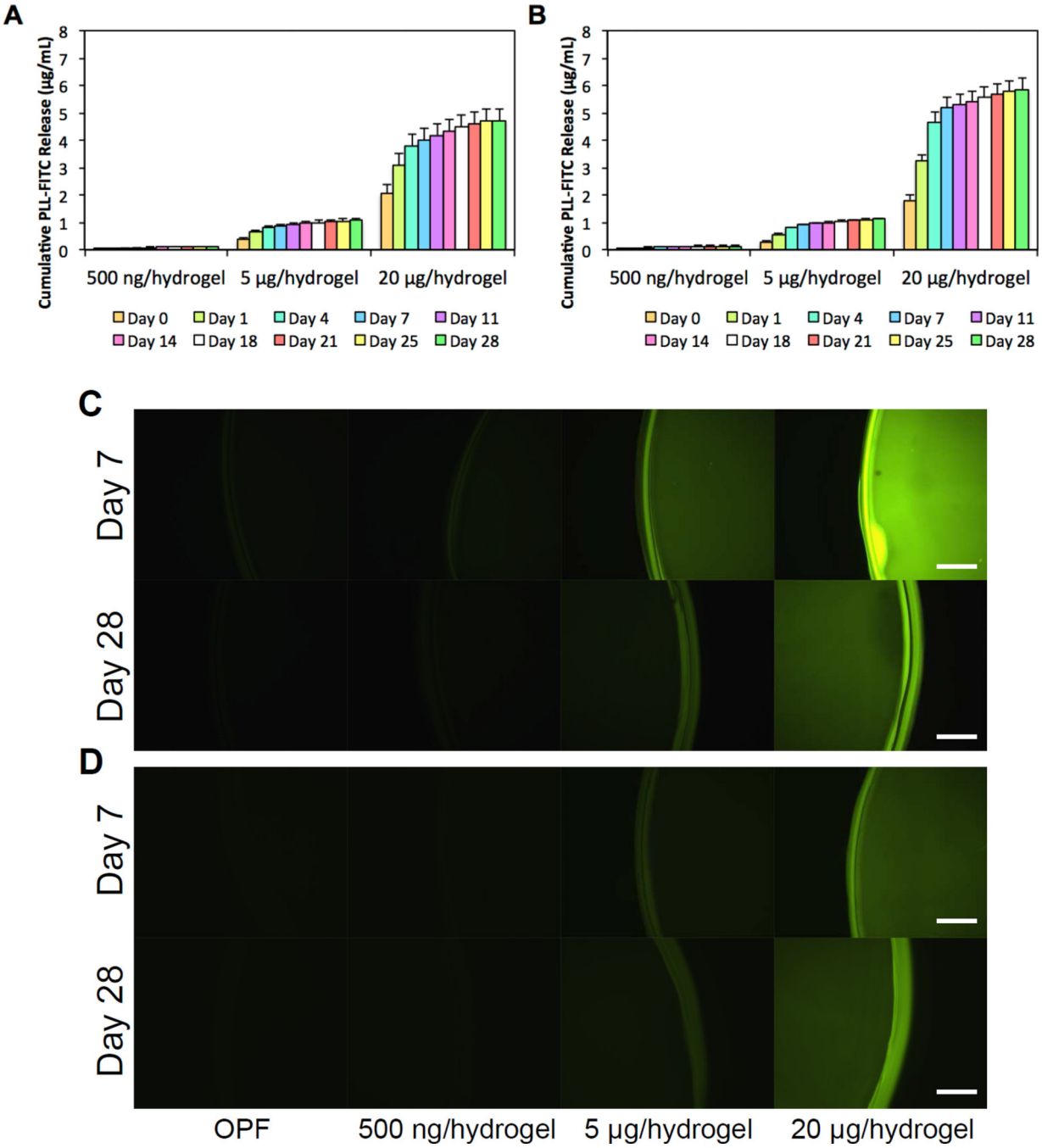

Figure 2.

Cumulative PLL-FITC release from (A) 10K OPF hydrogels and (B) 35K OPF hydrogels loaded with PLL at 500 ng/hydrogel, 5 µg/hydrogel, or 20 µg/hydrogel over 28 days is shown. Visualization of uniformly distributed PLL-FITC loaded into hydrogel constructs at each concentration, which is shown at days 7 and 28 after incorporation for (C) 10K hydrogels and (D) 35K hydrogels. Scale bar = 200 µm.

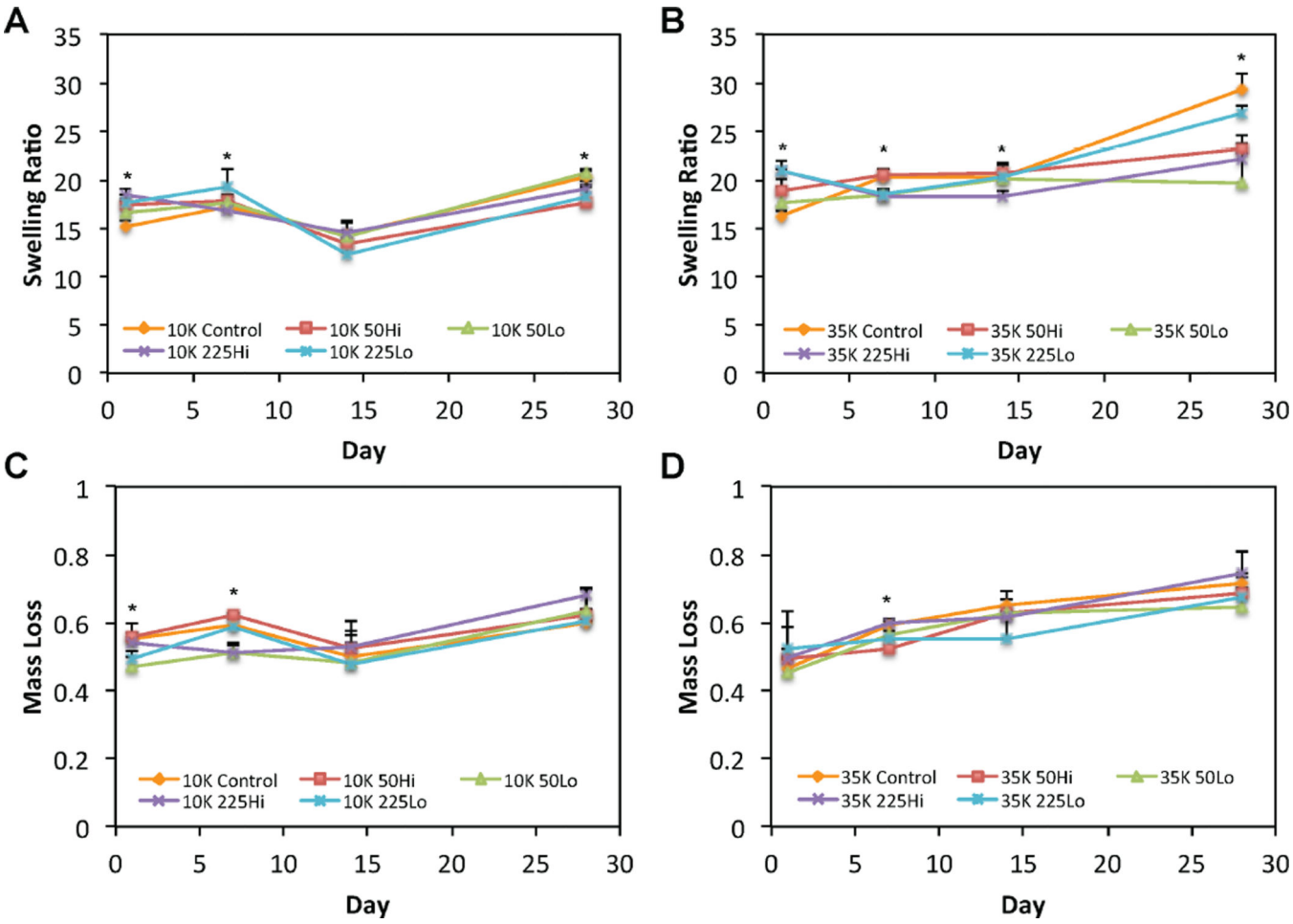

Figure 3.

Swelling ratio profiles are shown for (A) 10K OPF or (B) 35K OPF hydrogel formulations over 28 days. The mass loss profiles are shown for (C) 10K OPF or (D) 35K OPF hydrogel formulations over 28 days. The * indicates a difference between the 10K OPF or 35K OPF blank control group and at least one of the corresponding PLL-laden groups at that time point. Error bars represent the standard deviation (n=4).

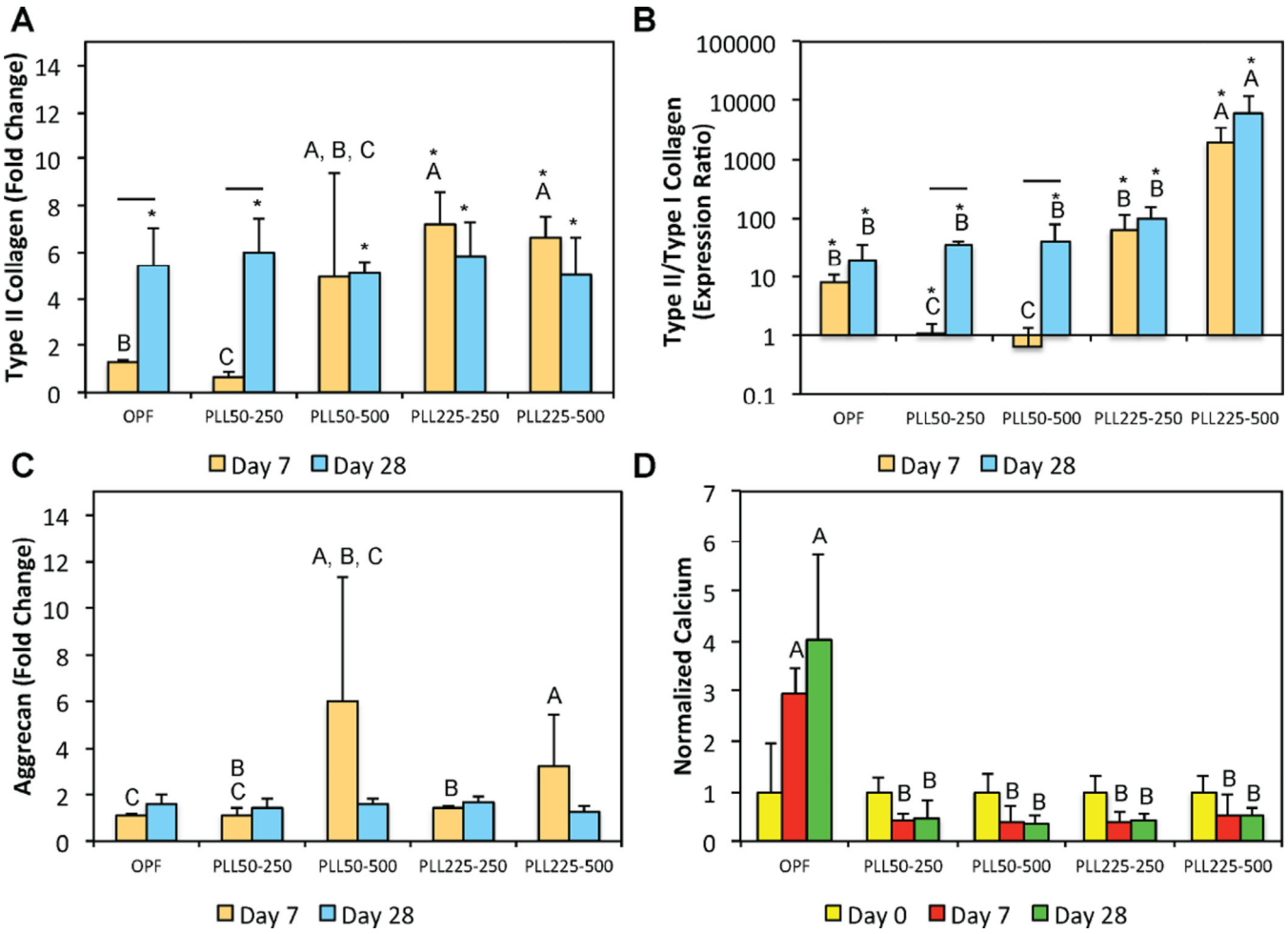

Figure 4.

Quantitative gene expression is shown for (A) type II collagen expression, (B) type II/type I collagen expression ratio, and the (C) aggrecan expression at days 7 and 28 for the first cell encapsulation study. The type II/type I collagen expression ratio is shown using a logarithmic scale for the y-axis. (D) The normalized calcium content at various time points. At each individual time point, groups not connected by the same letter are significantly different ($p<0.05$). Comparing time points within each individual group, time points connected by a bar are significantly different ($p<0.05$). The * indicates a significant difference when compared to the day 0 value of that corresponding group ($p<0.05$). Error bars represent the standard deviation (n=4).

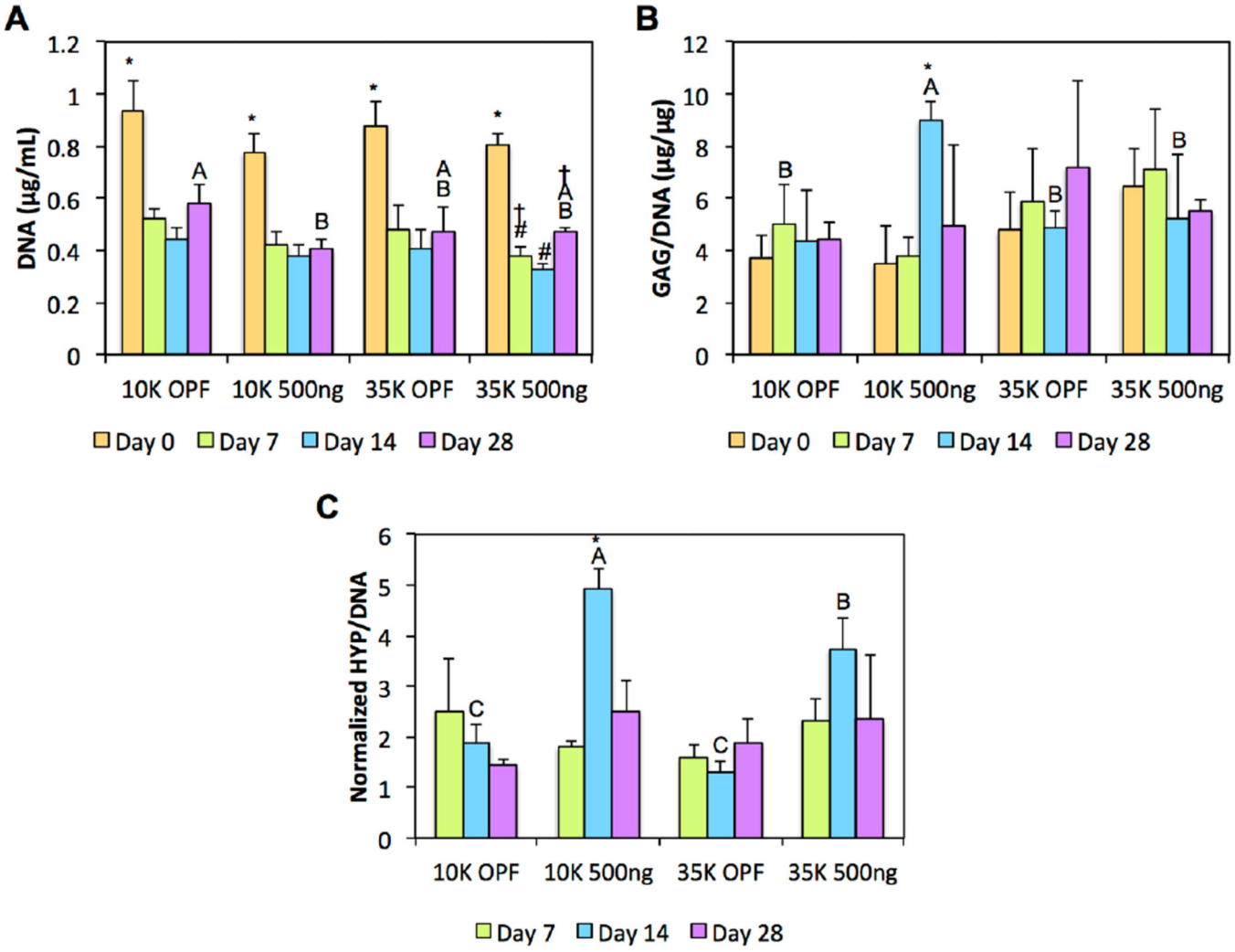

Figure 5.

(A) DNA content, (B) GAG synthetic activity, and (C) HYP synthetic activity of cell-laden composite hydrogels are shown at various time points. At each individual time point, groups not connected by the same letter are significantly different ($p<0.05$). Within each group at each individual time point, time points not connected by the same symbol are significantly different ($p<0.05$). Error bars represent the standard deviation (n=4).

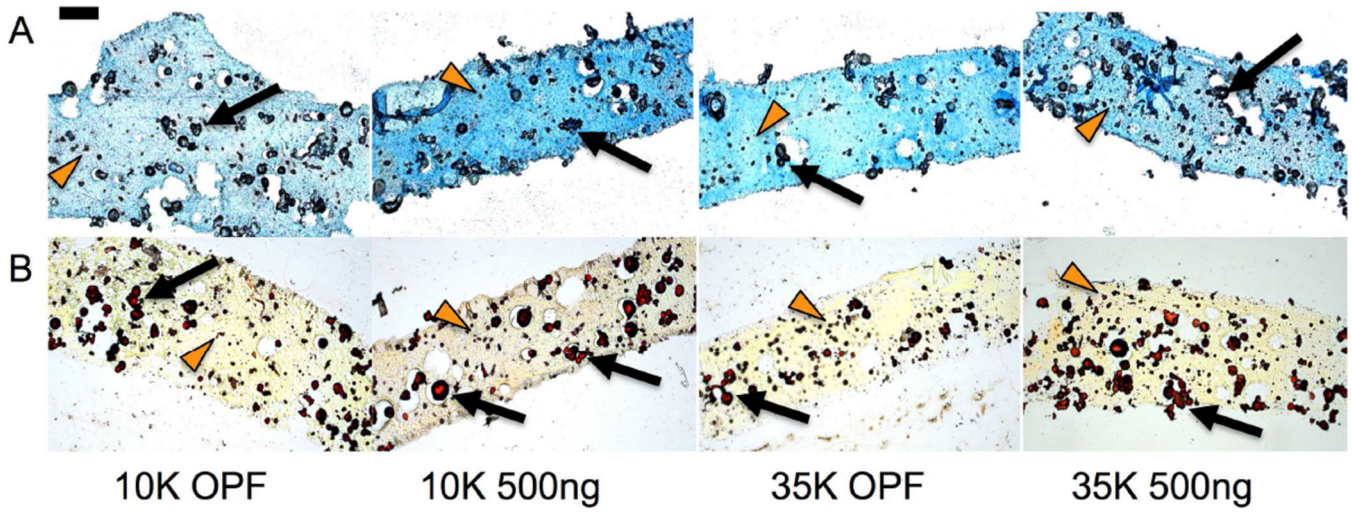

Figure 6.

Histological evaluation of GAG production using (A) Alcian Blue, where increasing shades of blue indicate greater sulfated GAG deposition, and collagen production using (B) Picrosirius Red, where increasing shades of red/orange indicate greater collagen deposition, are shown at day 14. GMPs and encapsulated MSCs are indicated with black arrows and orange arrowheads, respectively. Scale bar represents 200 μm for all images.

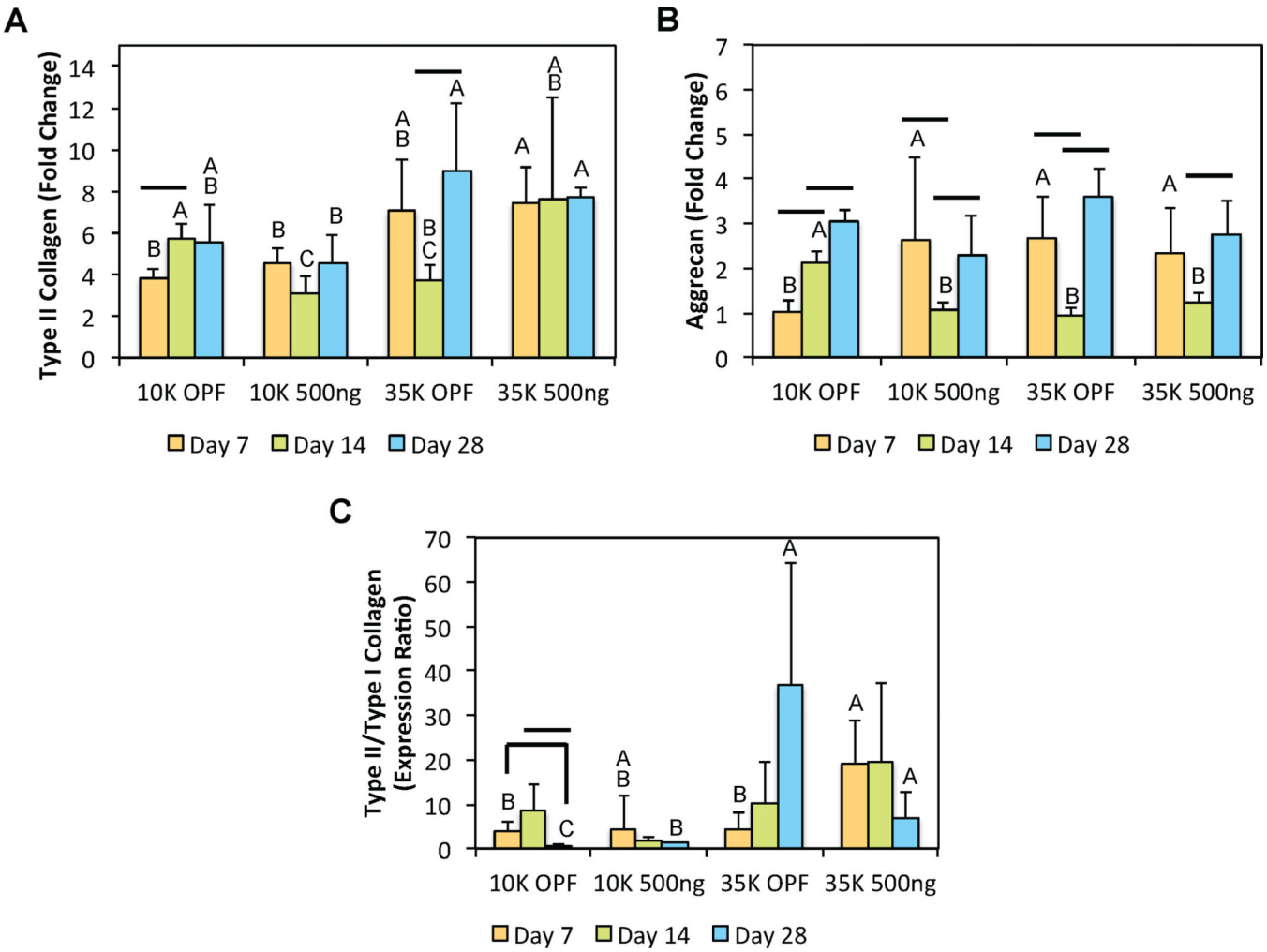

Figure 7.

Quantitative gene expression is shown for (A) type II collagen, (B) aggrecan, and the (C) type II/type I collagen expression ratio at various time points for the second cell encapsulation study. At each individual time point, groups not connected by the same letter are significantly different ($p<0.05$). Comparing time points within each individual group, time points connected by a bar are significantly different ($p<0.05$). Error bars represent the standard deviation (n=4).

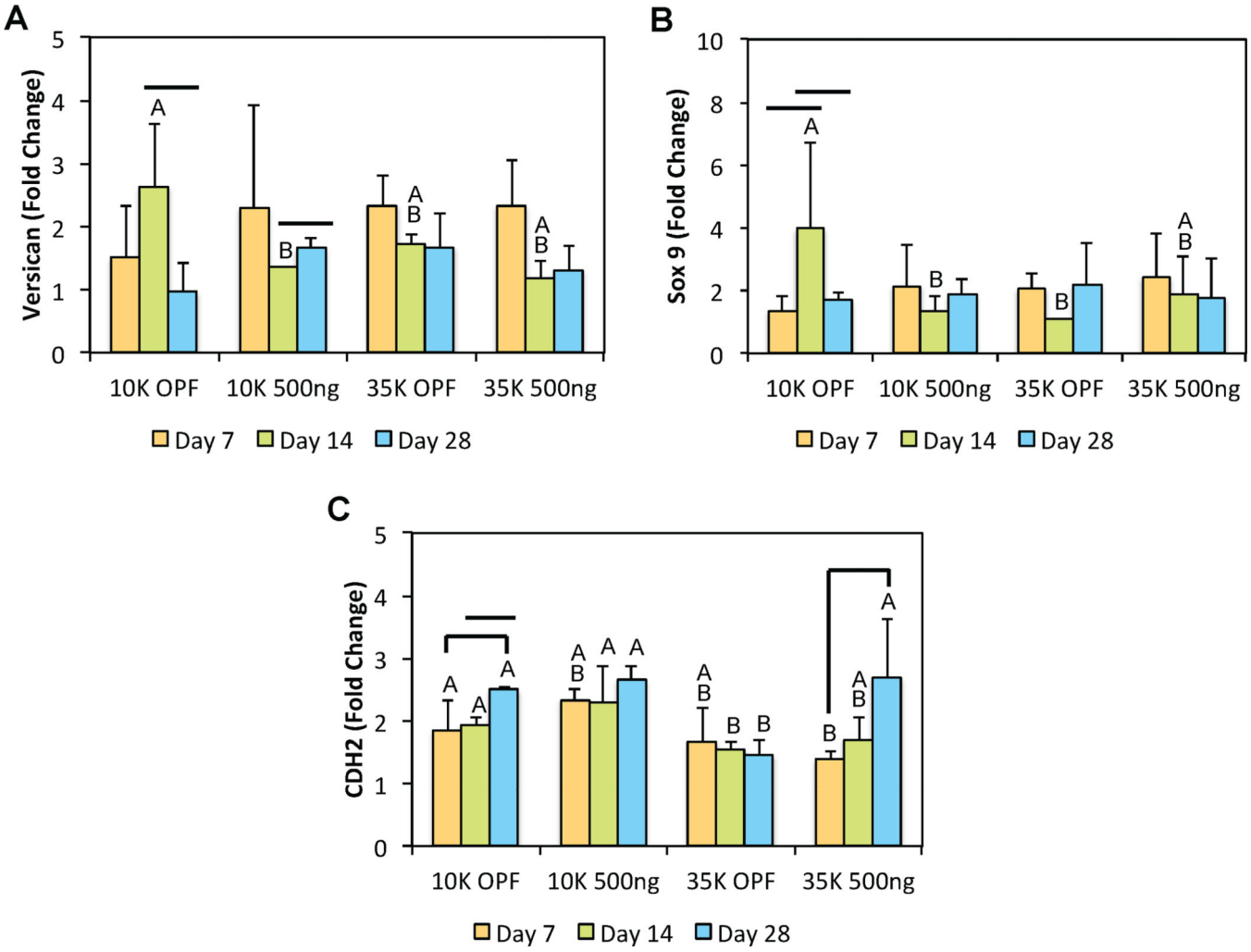

Figure 8.

Quantitative gene expression is shown for (A) Versican, (B) Sox9, and (C) CDH2 at various time points for the second cell encapsulation study. At each individual time point, groups not connected by the same letter are significantly different ($p<0.05$). Comparing time points within each individual group, time points connected by a bar are significantly different ($p<0.05$). Error bars represent the standard deviation (n=4).

Table 1

Experimental Design for the Determination of PLL Retention

i.	Group (n=3)	Incubation Condition	PLL Loading Method	PLL Dosage (μg/hydrogel)
	OPF	pH 7.4, 13	--	--
	OPF-Pre	pH 7.4, 13	During Fabrication	20
	OPF-Post	pH 7.4, 13	After Fabrication	20
ii.	**Group (n=3)**	**Incubation Condition**	**PLL Loading Method**	**PLL Dosage (μg/hydrogel)**
	OPF	pH 7.4	--	--
	OPF-Pre	pH 7.4	During Fabrication	20

i.) Samples were incubated at both pH conditions in parallel, and supernatants were collected and analyzed at 2 and 24 h post-fabrication. ii.) Supernatants were collected at 2 h, 1, 7, 14, and 21 days for analysis. Samples were then transferred to pH 13 incubation conditions for 24 h before collection and analysis.

Table 2

Experimental Design for the Determination of PLL-FITC Release

Group (n=3)	OPF MW (g/mol)	PLL MW (kDa)	PLL Dosage (per hydrogel)
OPF	10K, 35K	50	--
OPF-500ng	10K, 35K	50	500 ng
OPF-5μg	10K, 35K	50	5 μg
OPF-20μg	10K, 35K	50	20 μg

Table 3

Full Factorial Study to Characterize Swelling Behavior and Degradation of PLL-Laden Hydrogels

Levels (n=4)	(A) PLL MW (kDa)	(B) PLL Dosage (per hydrogel)	(C) OPF MW (g/mol)
Hi	225	20 μg	35K
Lo	50	500 ng	10K

PLL-free 10K and 35K OPF hydrogels were utilized as negative controls.

Table 4

Cell Encapsulation Study to Characterize the Effects of PLL Size and Dosage on Chondrogenic Gene Expression

Group (n=4)	PLL MW (kDa)	PLL Dosage (ng per hydrogel)
OPF	--	--
PLL50–250	50	250
PLL225–250	225	250
PLL50–500	50	500
PLL225–500	225	500

Table 5

Cell Encapsulation Study to Characterize the Effects of OPF Size and PLL Presentation on Chondrogenic Gene Expression and Condensation

Group (n=4)	PLL MW and Dosage	OPF MW (g/mol)
10K OPF	--	10K
35K OPF	--	35K
10K 500ng	225 kDa; 500 ng/hydrogel	10K
35K 500ng	225 kDa; 500 ng/hydrogel	35K

Table 6

Primer Sequences Used for Quantitative RT-PCR

Gene	Primer Sequence
Type II Collagen	5'-CTGCAGCACGGTATAGGTGA-3'
	5'-AACACTGCCAACGTCC AGAT-3'
Type I Collagen	5'-AGCAGACGCATGAAGGCAAG-3'
	5'-CCCAGAATGGAGCAGTGGTTA-3'
Aggrecan	5'-CGTAAAAGACCTCACCCTCCA-3'
	5'-GCTACGGAGACAAGGATGAGT-3'
Versican (VSN)	5'-GCTACACCCTTCCCATCAGT-3'
	5'-GAATTTGCTCTGAGGAAGCC-3'
Sox9	5'-GAGCGAAGAGGACAAGTTCC-3'
	5'-GTCCAGTCGTAGCCCTTGAG-3'
Type X Collagen	5'-ATGGAGTGTTCTACGCTGAG-3'
	5'-CCTCTCACTGGTATACCTTTACT-3'
N-Cadherin (CDH2)	5'-CTGCTATTGATGCGGATGAC-3'
	5'-TGAACATGTTGGGAGAAGGA-3'
GAPDH	5'-TCACCATC TTCCAGGAGCGA-3'
	5' -CACAATGCCGAAGTGGTCGT-3'